Earable Multimodal Sensing and Stimulation: A Prospective Toward Unobtrusive Closed-Loop Biofeedback

Yuchen Xu, Abhinav Uppal, *Graduate Student Member, IEEE*, Min Suk Lee, Kuldeep Mahato, Brian L. Wuerstle, Muyang Lin, Omeed Djassemi, Tao Chen, Rui Lin, Akshay Paul, Soumil Jain, *Member, IEEE*, Florian Chapotot, Esra Tasali, Patrick Mercier, Sheng Xu, Joseph Wang, and Gert Cauwenberghs, *Fellow, IEEE*

(Methodological Review)

***Abstract*—The human ear has emerged as a bidirectional gateway to the brain's and body's signals. Recent advances in around-the-ear and in-ear sensors have enabled the assessment of biomarkers and physiomarkers derived from brain and cardiac activity using ear-electroencephalography (ear-EEG), photoplethysmography (ear-PPG), and chemical sensing of analytes from the ear, with ear-EEG having been taken beyond-the-lab to outer space. Parallel advances in non-invasive and minimally invasive brain stimulation techniques have leveraged the ear's access to two cranial nerves to modulate brain and body activity. The vestibulocochlear nerve stimulates the auditory cortex and limbic system with sound, while the auricular branch of the vagus nerve indirectly but significantly couples to the autonomic nervous system and cardiac output. Acoustic and current mode stimuli delivered using discreet and unobtrusive earables are an active area of research, aiming to make biofeedback and bioelectronic medicine deliverable outside of the clinic, with remote and continuous monitoring of therapeutic responsivity and long-term adaptation. Leveraging recent advances in ear-EEG, transcutaneous auricular vagus nerve stimulation (taVNS), and unobtrusive acoustic stimulation, we review accumulating evidence that combines their potential into an integrated earable platform for closed-loop multimodal sensing and neuromodulation, towards personalized and holistic therapies that are near, in- and around-the-ear.**

***Index Terms*—Earables, ear-EEG, ear-PPG, biofeedback, auditory neurofeedback, transcutaneous auricular vagus nerve stimulation, closed-loop neuromodulation.**

Manuscript received 4 September 2024; revised 10 November 2024; accepted 17 November 2024. Date of publication; date of current version. This work was supported by the UCSD Center for Wearable Sensors. *(Yuchen Xu, Abhinav Uppal and Min Suk Lee contributed equally to this work.) (Corresponding author: Gert Cauwenberghs.)*

Yuchen Xu is with the Institute for Neural Computation, University of California, San Diego, CA 92093-0523 USA, and also with the Aizip Inc., Cupertino, CA 95014 USA.

Abhinav Uppal, Min Suk Lee, Omeed Djassemi, Soumil Jain, and Gert Cauwenberghs are with the Shu Chien-Gene Lay Department of Bioengineering, University of California, San Diego, CA 92093-0412 USA (e-mail: gcauwenberghs@ucsd.edu).

Kuldeep Mahato, Muyang Lin, Sheng Xu, and Joseph Wang are with the Aiiso Yufeng Li Family Department of Chemical and Nano Engineering, University of California, San Diego, CA 92093-0448 USA.

Brian L. Wuerstle and Patrick Mercier are with the Department of Electrical and Computer Engineering, University of California, San Diego, CA 92093 USA.

Tao Chen is with the Department of Computer Science, University of Pittsburgh, Pittsburgh, PA 15260-9150 USA.

Rui Lin is with the Institute of Transportation Studies, University of California, Berkeley, CA 94720 USA.

Akshay Paul is with the Institute for Neural Computation, University of California, San Diego, CA 92093-0523 USA.

Florian Chapotot and Esra Tasali are with the Department of Medicine, University of Chicago, Chicago, IL 60637 USA.

Digital Object Identifier 10.1109/RBME.2024.3508713

I. Introduction

EARABLES or hearables [1], [2] are devices that can be worn inside or around the ears, and that provide additional functionality beyond audio input and output [3]. Earables have emerged as a transformative innovation in the domain of wearable health monitoring [4], [5], and as a neuromodulation platform for applying non-invasive stimulation to remedy a target pathology, such as using bimodal therapy combining auditory and electrical stimulation to the ear, with the goal of inducing plasticity in the auditory cortex of tinnitus patients [6].

Because of its anatomy and physiology, the ear is uniquely positioned for multimodal sensing. It provides access to sounds and vibrations in the ear, to a rich network of vasculature and innervation [5], [7], [8], [9], to the eyes [10], [11], [12], [13], [14], to the muscles of the jaw [14], and to the brain [15], [16], [17], [18], especially the temporal cortex [19], [20]. This opens the door to acoustic, optical, electrophysiological (ExG), and electrochemical sensing. The semi-flexible cartilage of the auricle (outer ear) provides a convenient structure for comfortably supporting in-ear and around-the-ear devices. Ubiquitious examples such as wireless earbuds and hearing aids demonstrate that earables are stable and suitable for extended wearability. In particular, ear electroencephalography (ear-EEG) technology has even been taken into orbit for sleep monitoring on the Huginn space mission [21].

With over a decade since the first report of the ear-EEG sensing concept [22], the ear electrography (ear-ExG) field has accumulated over 250 publications as of August 2024 (as seen by searching the Web of Science database for "ear-eeg OR ear-ppg OR ear-ecg OR ear-eog OR around-the-ear EEG OR behind-the-ear EEG"). As a sampling of the rich and growing ear-ExG literature, studies have reported innovations in sensor designs [13], [17], [23], [24], [25], [26], [27], [28], [29], [30], [31], [32], [33], [34], and custom integrated circuits and data acquisition systems optimized for ear-EEG [35], [36], [37], [38], [39]. Characterization and validation studies have performed simultaneous ear-EEG and scalp-EEG recordings [16], [19], [40], or used phantom models [41] and computational forward models to characterize the signal propagation from cardiac or cortical sources to the ear [19], [20], [42], [43], [44]. Recent reports of ear-EEG applications have included sleep staging [45], [46], [47], [48], [49], [50], epilepsy monitoring [51], [52], [53], brain-computer interfaces using speech imagery [54] or steady-state visual evoked potentials (SSVEP) [55], [56], [57], [58], audiometric assessment [59], and auditory attention decoding [60], [61] towards neuro-steered hearing aids [62].

Recent reviews are available that summarize the sensing capabilities of earables: Röddiger et al. [3] organized earables research by fundamental phenomenon that can be sensed from the ears, spanning physiological and health-related sensing, acivity-monitoring, human-computer interaction, and biometric applications. Masè et al. [5] reviewed in-ear hearables measuring body temperature, pulse rate, and blood oxygen saturation. Ne et al. [63] extended this criterion to hearables acquiring electrophsyiological signals. For the subset of earables research focusing on ear-EEG, Kaongoen et al. [64] reviewed ear-EEG studies including applications and analysis methods. Juez et al. [65] further narrowed their focus to in-ear EEG studies (that is, excluding around-the-ear devices), tabulating biomarkers validated against scalp-EEG, along with in-ear EEG applications and computational modeling approaches.

In addition to robust sensing, the ear provides opportunities to deliver stimuli for modulating brain and body activity. Two stimulation modalities well-suited to the ear are acoustic (sound) or electric (current) given its access to multiple cranial nerves, leading to downstream modulation of the brainstem and higher areas, often resulting in measurable biomarkers to gauge the effectiveness of the therapy or responsiveness of subjects. Given this duality of stimulating sensory nerves and sensing downstream effects from the brain and body, Ruhnau and Zaehle wrote a perspective in 2021 [66] suggesting that ear-EEG could be combined with transcutaneous auricular vagus nerve stimulation (taVNS) in a wearable, closed-loop neuromodulation device targeting alpha activity as a biomarker of attention. Although the design or validation of such a device has not been reported in the literature thus far, and the modulation of alpha activity has had mixed reports given the evolving mechanistic understanding of the field [67], [68]. Our goal, as highlighted in Fig. 1, is to position earables as a more comprehensive approach, with multimodal sensing of brain and body activity, integrated with bimodal stimulation capability leveraging the ear's access to both the aurciular branch of the vagus nerve (ABVN) and the vestibocochlear (auditory) nerve.

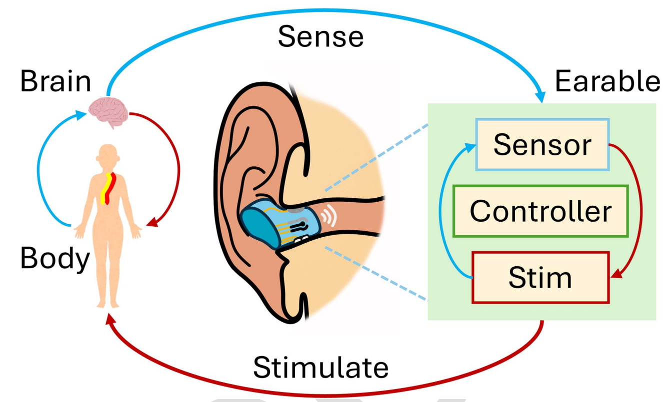

Fig. 1. Overview of a biofeedback earable system. Left: the brain and body form a closed-loop control system using electrical and chemical messaging through neuronal and vascular networks. Right: components of the earable, consisting of sensing and stimulation (Stim) systems, also form a closed-loop control system for adapting the stimulation given sensed changes in the user's state, thus providing biofeedback to the user.

The rest of this paper is organized as follows: Section II enumerates the anatomical and physiological properties of the ear to highlight its unique access to a plethora of physiological and neural signals. Sections III and IV provide the necessary background for sensing and stimulation principles, respectively, as applicable for various modalities in the ear. Section V provides an overview of considerations for system-level integration in earables. Section VI develops key steps towards closing the loop between earable sensing and stimulation, followed by our conclusions in Section VII.

II. Ear as a Bidirectional Gateway

The human ear's unique anatomical and physiological properties make it an ideal site for various sensing modalities. Beyond its primary role in hearing, the ear's structure, location, and vascularization offer significant advantages for physiological, chemical, and brain activity monitoring. This section briefly highlights how these characteristics enable multiple sensing opportunities.

Fig. 2 shows an input-output (I/O) map of the ear, with a rich diversity of inputs that can be provided to the ear as stimuli, and outputs that can be sensed from the ear. The following sub-sections highlight some key enabling features that uniquely position the ear for both sensing from and stimulating the brain and body.

A. Biosignals

1) Proximity to the Brain: The ear's closeness to the brain makes it an optimal site for monitoring neural activity through biopotential electrodes. This proximity minimizes signal degradation and allows for the detection of brain waves with higher fidelity compared to peripherally worn sensors (wrist-watches, finger tips, chest straps, etc).

2) Stable Blood Flow: The ear's robust vascularization and lower susceptibility to peripheral vasoconstriction, compared to the limbs, is advantageous for photoplethysmography (PPG)

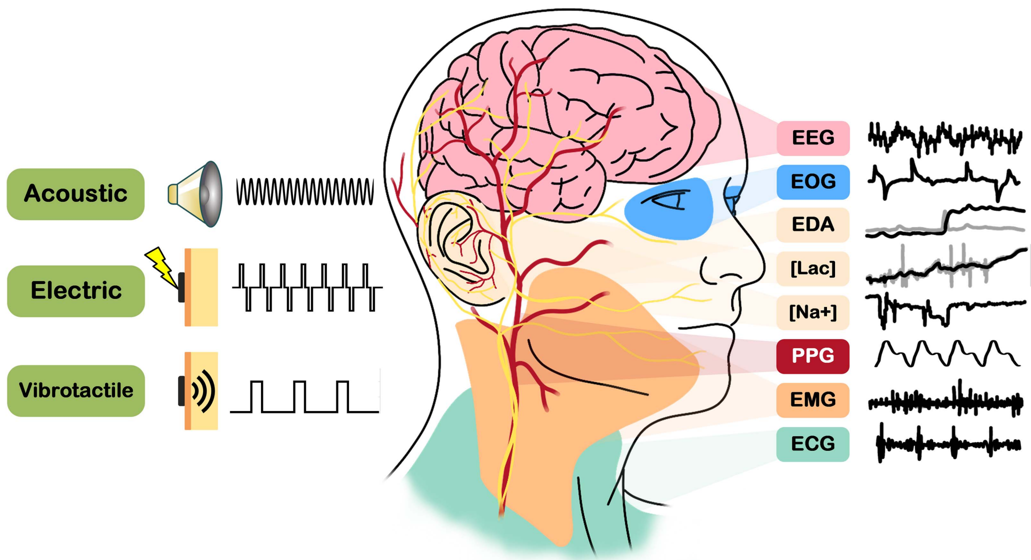

Fig. 2. The human ear as a bidirectional gateway to brain and body signals. Left: examples of sensory stimulation that can be delivered through the ear include acoustic, electric, and vibrotactile stimuli. Center: the ear provides access to innervation for delivering stimuli, and its proximity to vasculature and multiple sources of biosignals enable sensing. Right: examples of brain and physiological signals, with colors corresponding to sources of origin. EEG: electroencephalogram, EOG: electrooculogram, EDA: electrodermal activity, Lac: lactate, Na^+ : sodium, PPG: photoplethysmogram, EMG: electromyogram, and ECG: electrocardiogram.

sensors measuring heart rate and oxygen saturation. This stability ensures consistent readings even under varying environmental conditions.

B. Stability

1) Minimal Motion Artifacts: Compared to other body parts, the ear remains relatively stable due to less muscle movement and natural damping of vibrations due to the structure of the skull. Additionally, the placement of the sensors in the ear provides better protection from external environmental factors. However, the ears are still subject to certain movements such as chewing or talking. In order to mitigate these artifacts for mobile brain imaging (MoBI), careful sensor design [69], [70], [71], [72], [73] and sensor placement [14], [74], [75] are needed to increase measurement accuracy and reduce post-processing requirements for artifact removal.

2) Mechanical Anchoring Point: The ear provides a natural and secure anchoring point for wearable devices. The pinna's grooves allow for stable attachment of sensors and devices without the need for additional securing mechanisms. This mechanical anchoring ensures that the devices remain in place during various activities, enhancing the reliability of the collected data.

C. User Adoption

1) Pervasiveness and Social Acceptability of Earphones: The widespread use of earphones and their social acceptance in daily life make the ear a familiar and non-intrusive location for future earables that can maintain the earphone form-factor. Users are accustomed to wearing devices in their ears, which improves compliance with experimental protocols and retention over longer studies.

2) Comfortable and Discreet Placement: Earables are generally more comfortable for long-term wear, compared to other body-worn sensors like headset, chest straps or wristbands, which requires minimal adjustment and are less intrusive to daily activities. Their discreet placement within/near the ear canal or around-the-ear makes them less noticeable to others, alleviating any social awkwardness often associated with conventional EEG systems.

D. Innervation

The ear's access to multiple sensory nerves including the vestibulocochlear nerve carrying acoustic, motion, and positioning information, and the auricular branch of the vagus nerve (ABVN) carrying somatosensory information allow for acoustic, electric, and bimodal stimulation of the brainstem and higher brain areas, that can induce electrical, chemical (through neurotransmitters), and physiological changes (by modulating the cardiac system).

III. Multimodal Earable Sensing

As mentioned in Section II, the ears offer unique advantages over other body parts due to the ear's distinct anatomical and physiological characteristics. This section focuses on sensing technologies for earables, comparing ear-based sensing with sensing from other common body parts such as the scalp, arm, chest, wrist, fingers, and legs.

A. Electrophysiological Sensing

Neurophysiological sensing systems are essential for monitoring and understanding the electrical activities of the nervous system. These systems utilize various modalities to capture brain activity, muscle activity, and eye movements, providing valuable insights into cognitive functions, motor control, and sensory processing. The primary sensors used in wearable neurophysiological sensing systems are biopotential electrodes [77], which detect electrical potentials generated by neural and muscular activity. These electrodes are commonly made from materials like silver/silver chloride (Ag/AgCl), and are designed to ensure a stable and reliable interface between the skin and the sensor.

Electrography (ExG) encompasses a range of techniques, including electroencephalography (EEG), electromyography (EMG), electrocardiography (ECG), and electrooculography (EOG), which measure the electrical activity of the brain, muscles, heart, and eyes, respectively. In addition to these ExG signals, electrodermal activity (EDA) can also be measured using the same electrophysiological measurement setup. EDA characterizes the skin's conductance response [78], which varies with sweat gland activity and is commonly associated with physiological arousal and stress levels. These techniques rely on biopotential electrodes that are placed on the skin's surface to detect small biopotentials generated by neural or muscular activity. The electrodes capture these signals, which are then amplified, filtered, and digitally recorded for analysis. A differential architecture is often used to minimize noise and interference by comparing signals from paired electrodes, forming a bipolar channel for more accurate measurement. The feasibility of using ear biopotential sensors to measure ExG has been validated by previous research with simultaneous recording of comparison data from reference locations such as the scalp (EEG), chest (ECG), and finger (PPG) [5], [63].

Each type of ExG signal has distinct characteristics. EEG signals, typically ranging from 20 to 150 μV with a bandwidth of 0.5–60 Hz, reflect the brain's electrical activity and vary both temporally and spatially across the scalp [79]. EMG signals, which are generally larger than EEG signals, capture the electrical activity of muscles during contraction, with amplitudes ranging from a few microvolts to millivolts, and bandwidths typically between 10 Hz and 500 Hz [38]. EOG signals, used to measure eye movements, fall within the range of 0.1 to 5 mV with a bandwidth of 0–35 Hz, reflecting the potential differences generated by eye movements. EOG signals can be further categorized based on their origin: eye blinks and eye movements. Eye blinks produce transient, high-amplitude signals that are typically short in duration, while eye movements generate more sustained signals with lower amplitudes [80]. Together, these ExG modalities provide a comprehensive approach to monitoring and analyzing various physiological processes.

1) Biopotential Sensors: Electrodes for electrophysiology are conductive materials that enable electrical conduction between the subject and the recording electronics. However, the choice of electrode affects the design, durability, maintenance, biocompatibility, signal quality, comfort, longevity, usability, and other features. Such considerations are especially important when devising miniaturized wearables such as ear-EEG devices [53], [78].

Biopotential electrodes including widely used Ag/AgCl electrodes capture EEG signals through the electrochemical interface between the electrode surface and the skin. When neurons in the brain fire, they produce electrical signals that propagate through the brain and skull, reaching the surface of the scalp and the ear. Biopotential electrodes convert these ionic currents in the body to electronic currents that can be measured. The Ag/AgCl material is particularly effective due to its low and stable impedance, and high signal fidelity, making it suitable for picking up the relatively weak EEG signals. The electrodes act as transducers, capturing the voltage fluctuations caused by brain activity, which can then be amplified and recorded by the EEG system.

Currently, there are three major interface methods: gel, dry, and non-contact electrodes. Gel-contact utilizes conductive gel which ensures stable physical contact and lower impedance. Previous work has demonstrated stable and low electrode-skin impedance values maintained for several hours using cEEGrids, where adhesive tape seals the electrode-skin interface, minimizing air exposure and preventing the gel from drying out, thus allowing prolonged recording sessions [81]. Such configurations are particularly suitable in clinical or research settings where stable, high-quality signals are prioritized. However, these systems often require extended maintenance, cleaning, and careful application to achieve optimal results.

For user comfort and ease of long-term use, especially in wearable applications, a system that operates without adhesives and gel would be more ideal, minimizing discomfort and simplifying usability. Dry-contact electrodes do not require conductive gel, but still have conductive material directly in contact with the skin. Such electrodes are less obtrusive and more convenient for long-term recording. However, they typically have higher impedance than gel-based electrodes, and requiremechanical force or adhesives to fixate the electrodes on the skin to ensure good contact. This can often lead to discomfort.

Non-contact electrodes utilize capacitive coupling between conductive electrode material and the skin to detect electrical signals without physically touching the body [82], [83]. Similarly to dry-contact, non-contact enables ease-of-use, long-term monitoring, and reusability. Additionally, it can be considered more hygienic, which reduces skin irritation or infections due to the conductive material. However, non-contact has several cons: it typically has higher impedance than dry-contact, which leads to lower signal quality; it requires more complex electronics to amplify the signal; it is more prone to motion artifacts as the gap between the skin and the electrode may change due to movement, affecting the capacitance that the non-contact electrodes rely on.

Although there are these three contact options, in-ear EEG literature predominantly uses dry-contact. One of the major benefits of in-ear EEG is the eventual wearable applications for consumer use. Wet-contact electrode characteristics are not beneficial for ease-of-use and long-term recording. For non-contact, the ear devices typically have limited space, making it difficult to incorporate amplifiers needed to boost the signal. Additionally, wearables require mobility. Therefore, non-contact electrodes which are more susceptible to motion artifacts will make it less favorable for wearable applications [84]. Although dry

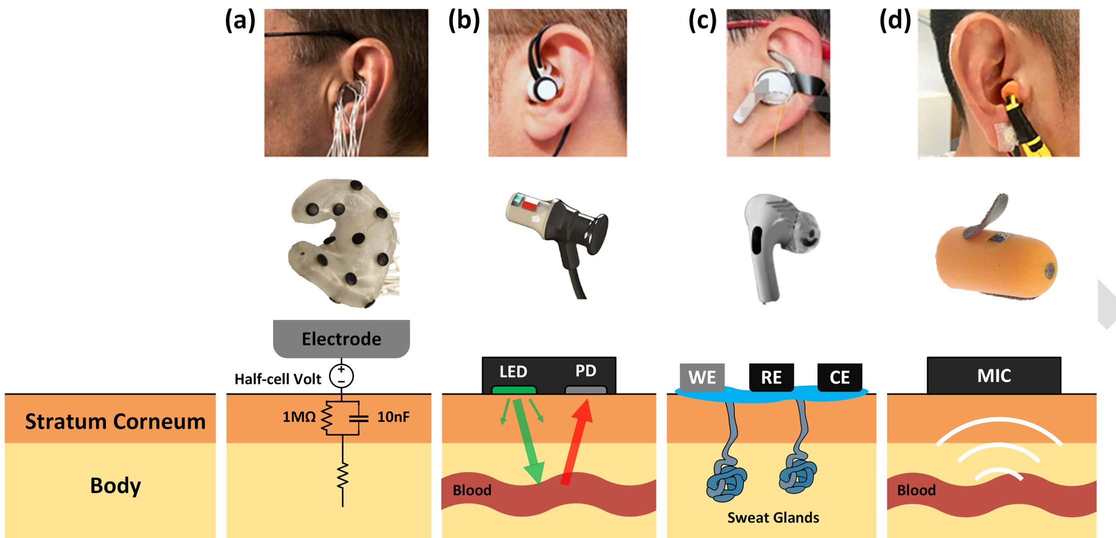

Fig. 3. An overview of earables for different sensing modalities. For all subfigures from bottom to top: physiological sources, illustrative devices, and devices as worn by users. Bottom row from left to right: (a) half-cell model of the skin-electrode interface for electrophysiological signals, (b) optical interface for pulse plethysmography consisting of a light-emitting diode (LED) and a photo detector (PD), (c) sweat glands generating chemical analytes, and (d) mechano-acoustic sources visualized as a pulsing artery (other possible sources of ear canal motion and vibrations including sound not shown). Sources of device images from left to right: (a) Kappel et al. [26], ©2017 IEEE, (b) Budidha and Kyriacou [76], (c) Xu et al. [13], (d) Goverdovsky et al. [1]. Device images (b)–(d) were modified to remove annotations, and are under the CC-BY 4.0 International License: http://creativecommons.org/licenses/by/4.0/.

contact requires mechanical pressure or adhesives to ensure good contact, the geometric enclosures of the ear enable mechanical fitting for stable fixture. Additionally, many studies and methods have also been performed to mechanically stably fit objects to the ear.

A dry-contact electrode model is illustrated at the bottom of the column Fig. 3(a). This model represents the skin-electrode interface as a combination of resistive and capacitive components that together form the overall impedance of the system [84]. The skin's resistive properties are represented by a resistance R_e (conductance $G_e = 1/R_e$). This resistance is a function of the electrode's contact area with the skin and the inherent resistivity of the skin's outer layer (stratum corneum). The capacitive component C_e arises from the dielectric properties of the skin and the insulating layer of the electrode. This capacitance is influenced by factors such as the dielectric constant of the skin, the thickness of the stratum corneum, and the distance between the electrode and the underlying conductive tissues. The capacitive coupling allows the electrode to detect biopotential signals even in the presence of a non-conductive layer, but it also introduces a frequency-dependent impedance. The total impedance at the skin-electrode interface is modeled as a parallel RC circuit:

$$Z_e = 1/(G_e + j\omega C_e). \tag{1}$$

The impedance at the skin-electrode interface directly influences the noise levels in the recorded signals. The importance of a low impedance of the skin-electrode interface is twofold; firstly, the impedance generates thermal noise as described by the Johnson-Nyquist equation. Secondly, the current noise of the amplifier is converted to voltage noise through the impedance [85]. Previous research show that the impedance of ear biopotential electrodes ranges from 1.2 MΩ at low frequencies to lower than 100 kΩ at high frequencies for dry electrodes, and from 34 kΩ at low frequencies to 5.1 kΩ at high frequencies for wet electrodes, characterized across a frequency range of 0.1 Hz to 2 kHz [85]. Another challenge in the ear is the variation of impedance at the ear electrode-skin interface due to environmental factors like cerumen presence and electrodermal activity [78], which requires careful consideration of biopotential sensor designs.

A key factor to affect the impedance of biopotential electrodes is the material. Key features for the electrode material should be low impedance and biocompatible. Low impedance will enable better signal quality and biocompatible will prevent toxic exposure to the user after prolonged skin contact and have hypoallergenic properties to minimize the risk of skin reactions. The types of materials used in literature for in-ear EEG are but not limited to conductive polymers [53], [86], gold [87], CNT/PDMS [88], IrO2 [27], [89], composite silicone, and predominantly, silver [13], [25], [90], [91], [92], [93], [94], [95], [96] and Ag/AgCl [22], [29], [38], [97], [98]. Additional features such as material flexibility, design/shape, durability and maintenance are important considerations that vary among sensors. The fabrication techniques of these sensors also widely vary yet are integral to optimize and balance these features. Examples found in literature for in-ear EEG sensors are electroplating [25], coating [13], [38], [53], [91], [92], [99], solid metal working [24], [27], [89], [95], [97], [98], conductive threading [25], [94], [100], [101], and molding [88]. Nevertheless, the choice of fabrication techniques should accommodate the unique anatomical features of the ear canal while ensuring high signal quality. Apart for the impedance, it is also crucial that the fabrication of in-ear EEG devices ensures no structures including edges that could potentially damage the ear canal. These geometrical constraints make designing low-contact impedance electrodes more challenging, as the need to ensure a safe fit can limit the surface area and optimal positioning required for maintaining stable, low impedance contact. Researchers have proposed different electrode designs that can adapt to the anatomy of different subjects by adding degrees of adaptability through mechanical designs [13], [39].

The contact impedance between the electrode and skin is typically measured using the electrical impedance spectroscopy (EIS) method [79], [88], [102]. This characterization involves using three-electrode or four-electrode measurement configurations, where electrodes with similar contact areas are placed at specific distances (e.g., 1cm apart) on a skin surface, such as the forearm, to simulate conditions similar to their intended application site or the phosphate-buffered saline (PBS) solution as a simulated environment. The impedance is measured across a range of frequencies, typically from 1 Hz to 1000 Hz, and the contact impedance is derived by measuring the current resulted from the applied voltage.

For ear-EEG measurements, three main types of electrodes are typically used: measuring electrodes, reference (REF) electrodes, and ground (GND) electrodes. Measuring electrodes are placed in [27] or around [81], [103] the ear to detect brain activity. The reference electrode provides a baseline for the measurements, ensuring that the signals from the measuring electrodes are recorded relative to a consistent point. The referencing configuration can be categorized as contralateral when the reference electrode is located at the opposite side of the sagittal plane from the measuring electrode or ipsilateral when it is placed within the same ear or surrounding area [104]. The ground electrode stabilizes the electrical environment by providing a common return path for the electrical current and reducing noise from external sources. For ear-EEG recordings REF and GND are usually located at the concha [31], [39], [104] or mastoid [99], [105]. For ear-ECG, due to the relatively farther distance to the source of signal, REF and GND are usually located non-cephalic to capture ECG signals of good quality [106]. Ear-ECG measured completely from the ear has also been explored. Single-ear ECG is feasible but challenging for cardiac rhythm monitoring. The limitations particularly are lower signal amplitude and higher susceptibility to noise compared to a cross-ear ECG setup, due to the smaller potential difference and closer proximity of electrodes, which reduce signal quality and reliability [42], [43].

2) ExG Signal Characteristics: Ear-ExG sensing employs similar sensing mechanisms to those ExG sensing from other parts of the body. However, ear-ExG mainly differs by its limited size and placement options, leading to differences in signal characteristics. To quantify these characteristics for ear-ExG sensing, previous research has built forward models to simulate the mapping of brain sources and compares the difference of electrical potential distributions between the scalp and ear [19], [107]. Forward models specifically refer to the transfer function from sources in the brain volume to biopotential electrodes. Here we describe using a simplified brain signal dipole model to illustrate such differences with the most widely reported ear-ExG sensing modality: ear-EEG. EEG signals are generated by the synchronous activity of large populations of neurons, primarily in the cerebral cortex. When neurons fire, they create current dipoles due to the movement of ions across cell membranes, generating an electrical field through volume conduction. This field can be described by the primary current source J and the secondary volume currents induced in the surrounding conductive medium (brain tissue, skull, scalp). Scalp or ear-EEG measures the potential difference between two points: the measuring electrode and the reference electrode. The potential $V(\mathbf{r})$ at an electrode placed at position $\mathbf{r}$ due to a current dipole source $\mathbf{p}$ at position $\mathbf{r_p}$ in an infinite, homogeneous medium with conductivity σ can be described by simplified dipole analysis [20] as shown in Fig. 4:

$$V(\mathbf{r}) = \frac{1}{4\pi\sigma}\,\mathbf{p}\cdot\frac{\mathbf{r}-\mathbf{r_p}}{\|\mathbf{r}-\mathbf{r_p}\|^3} \tag{2}$$

The potential difference measured by the ear or scalp-EEG setup between a measuring electrode at $\mathbf{r}$ and a reference electrode at $\mathbf{r}_{\text{ref}}$ is:

$$\begin{aligned}\Delta V &= \frac{1}{4\pi\sigma}\mathbf{p}\cdot\left(\frac{\mathbf{r}-\mathbf{r_p}}{\|\mathbf{r}-\mathbf{r_p}\|^3}-\frac{\mathbf{r}_{\text{ref}}-\mathbf{r_p}}{\|\mathbf{r}_{\text{ref}}-\mathbf{r_p}\|^3}\right)\\ &\approx \frac{1}{4\pi\sigma}\,\mathbf{p}\cdot\frac{\mathbf{r}-\mathbf{r}_{\text{ref}}}{\|\mathbf{r}-\mathbf{r_p}\|^3};\ \|\mathbf{r}-\mathbf{r}_{\text{ref}}\|\ll\|\mathbf{r}-\mathbf{r_p}\|\end{aligned} \tag{3}$$

from which we derive that distance and the angle between electrodes and dipole moment are the main factors for signal characteristics. A first and important consideration is that for closely spaced electrodes located far away from the source, the magnitude of the measured potential is directly proportional to the distance $D = \|\mathbf{r}-\mathbf{r}_{\text{ref}}\|$ between the electrodes. Specifically the signal amplitude decreases by a factor proportional to the relative difference, $\|\mathbf{r}-\mathbf{r}_{\text{ref}}\| / \|\mathbf{r}-\mathbf{r_p}\|$, which further depends on the orientation of the electrode geometry $\mathbf{r}-\mathbf{r}_{\text{ref}}$ relative to the dipole $\mathbf{p}$, producing a null in the measured signal where $\mathbf{r}-\mathbf{r}_{\text{ref}}$, rather than $\mathbf{r}-\mathbf{r_p}$, is perpendicular to $\mathbf{p}$. The implication for in-ear electrode geometries with mm-scale inter-electrode distances is that they can pick up signals originating from the cortical surface that are typically observed by scalp-EEG with cm-scale distances, but with attenuated signal levels further aggravated by higher noise levels due to smaller-size electrodes resulting in 10–20 dB loss in signal-to-noise dynamic range.

However, an equally important consideration is that ear-EEG is able to resolve signals different from scalp-EEG with greater specificity. Specifically, if $\mathbf{r}$ and $\mathbf{r}_{\text{ref}}$ are relatively closer to the source $\mathbf{r_p}$, the measured potential difference will be larger and more specific to the source. This preliminary analysis can be applied to contrast the relative merits of ear- and scalp-EEG. Scalp-EEG places electrodes over the entire scalp, providing a comprehensive view of brain activity, while ear-EEG electrodes are placed inside or around-the-ear, providing a "keyhole" view of activity from the temporal lobe [108]. The distance from cortical sources to ear electrodes is generally greater than the distance to scalp electrodes, potentially reducing signal amplitude in the ear. The exception here is the temporal lobe, which will be closer to the ear electrodes when placed in the ear canal. The angle of measurement is limited to the relative

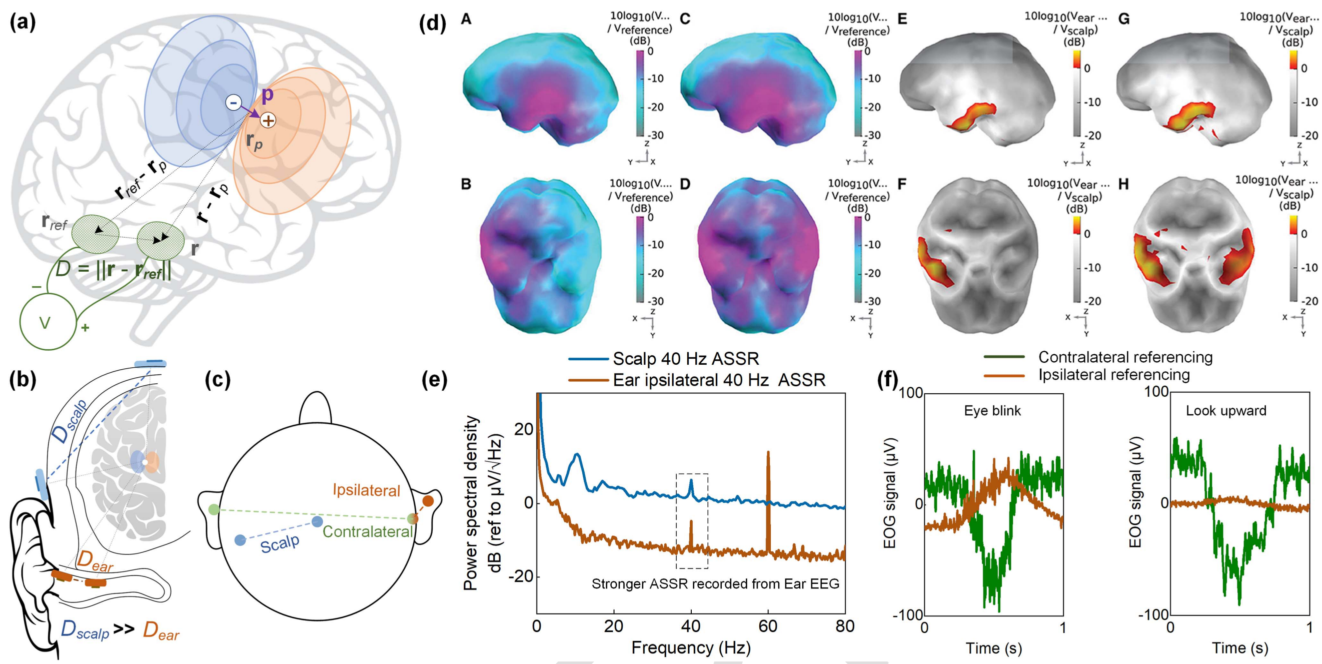

Fig. 4. Characteristics of brain ExG signals between the scalp and ear. (a) EEG is measured by placing electrodes on the surface of the scalp or in the ear to measure volume currents that yield potential differences. These potential differences are generated by a large number of simultaneously active neurons, which produce current dipoles across a small cortical area, often summarized as an equivalent current dipole. (b) Ear-EEG electrodes are placed in the ear canal or around the ear to measure the brain's electrical activity. The distance between the source and the measuring electrode is smaller than in scalp-EEG setups. While the distance between the ear-EEG electrodes and the source dipoles is generally larger than that of the scalp electrodes, there is an exception for signal sources from the auditory cortex on the same side as the ear-EEG electrodes. (c) Illustration of three common types of EEG measurement referencing setups. Scalp-EEG commonly employs references along the midline of the scalp (Cz shown in the figure) or mastoid. Ear-EEG commonly uses ipsilateral referencing, where the reference electrode is placed in the same ear as the measuring electrodes and contralateral referencing, where the reference electrode is placed in the opposite ear to the measuring electrodes. (d) Sensitivity map for brain sources analyzed by Yarici et al. [20]: (A), (B) Sensitivity map for a left ear unilateral (ipsilateral) ear-EEG montage. (C), (D) Sensitivity map for a bilateral (contralateral) ear-EEG montage. (E, F) Relative sensitivity map for a left ear unilateral montage and a 64-channel scalp-EEG montage. (G), (H) Relative sensitivity map for a bilateral ear-EEG montage and a 64-channel scalp-EEG montage. (A)–(D) The sensitivities displayed for each individual brain sources (dipoles) are extracted from the optimal differential pair of electrodes within the montage (for that dipole). High and low sensitivities are represented by magenta and cyan shading, respectively. (E)–(H) Severe and moderate signal losses are displayed in gray and white, respectively. Signal gains are displayed in red and yellow. (A), (C), (E), (G) Left brain surface. (B), (D), (F), (H) Inferior surface of the brain [20]. (e) Ear-EEG measurement data demonstrate that ear-EEG can pick up even stronger signals than scalp-EEG for sources close to the ear electrodes, such as the auditory cortex in the temporal lobe [13]. (f) Ear EOG measurement in ipsilateral and contralateral referencing. For eye blinks, both referencing setups record the blinking signal, while contralateral referencing records a much larger amplitude. For eyeball movement, ipsilateral referencing records very little signal component, while contralateral referencing records a much larger EOG amplitude [13]. Sensitivity maps A-H in subfigure (d) are ©2023 Yarici, Thornton and Mandic [20].

position of the ear, primarily capturing activity from lateral and inferior regions of the brain. The much smaller distance between electrodes also decreases the signal amplitude. The analysis here is in line with results from finite element modeling of the brain, which also indicates that ear-EEG only produces an increase in signal amplitude in limited regions in the temporal lobe, while adjacent regions mostly exhibited a moderate decrease in signal amplitude [19], [26]. It has also been shown that despite the limited spatial resolution and lower SNR of ear-EEG, there is a high degree of mutual information between signals captured by ear-EEG and those recorded by scalp-EEG [109].

The difference in amplitude between scalp and ear-EEG has significant implications for the design of sensors and analog front ends (AFE) used in earable EEG devices. The lower amplitude of ear-EEG signals necessitates the use of high-gain, low-noise amplifiers to ensure accurate and reliable signal capture. The gain required can be calculated using $G = V_{out}/V_{in}$, where V_{in} is the lower amplitude ear-EEG signal and V_{out} is the desired output voltage for the analog front end. Additionally, the signal-to-noise ratio (SNR) is a critical factor, given that ear-EEG signals are weaker, the SNR must be maximized by minimizing noise through the use of low-noise amplifiers, which have a low noise figure calculated as $NF = SNR_{in}/SNR_{out}$. In terms of the biopotential sensors, electrodes must have low impedance to ensure minimal signal loss and high-quality signal acquisition. The impedance of biopotential electrodes plays a critical role in the noise performance of earable systems. The thermal noise, which contributes significantly to the overall noise in such systems, can be modeled using the equation $V_{n\,rms}^2 = 4kT(G_e + G_{amp}) + V_n^2$. Here k is Boltzmann's constant, T is the absolute temperature, G_e is the skin-electrode coupling conductance from the skin-electrode impedance, G_{amp} is the amplifier input conductance, and V_n^2 is the input-referred noise of the amplifier. The reduction in noise is crucial for maintaining a high SNR in the AFE. High-resolution analog-to-digital converters (ADCs) are also necessary to accurately digitize the low-amplitude signals, with the resolution given by Resolution $= V_{\text{ref}}/2^n$, where V_{ref} is the reference voltage and n is the number of bits. The literature have shown that scalp-EEG signals typically range from 10 μV to 100 μV, while ear-EEG signals are usually lower, ranging from 1 μV to 10 μV [110]. This lower amplitude necessitates the use of high-gain amplifiers, with ear-EEG requiring a gain of 10 times more than the scalp-EEG. The noise figure for the amplifiers must be exceptionally low to maintain a high SNR due to the smaller signal amplitude of ear-EEG [111]. From an energy standpoint, driven by these requirements of the analog front-end earable sensing systems typically need to maintain a low noise efficiency factor (NEF) to reduce energy consumption while preserving signal fidelity. The higher resolution required by the ADC also asks for optimization of the energy per conversion level figure of merit (FoM) to balance energy efficiency with the need for accurate digitization of low-amplitude signals.

3) Ear-EEG Devices: Kaongoen et al. [64] have previously noted the variability in nomenclature in the ear-EEG field. In this review, we use "in- and around-the-ear EEG" shortened to "ear-EEG" to jointly refer to the devices and methods for recording EEG from inside and close to the external ear. When there is a need to refer to only one of these two sub-sets, we use "in-ear EEG" to describe sensors that fit within the auricle of the ear (see Looney et al. [22] for an early example), and "around-the-ear EEG" for devices that contact the hairless scalp behind the ear (for example, the device from Debener et al. [17]). Whereas around-the-ear EEG devices typically use electrode gel to make wet contact with the skin, in-ear devices have been reported as being wet- [15] or dry-contact [27], depending on whether electrode gel is applied before recording. We also note that electrode gel should not be assumed to refer to hydrogel, as alternatives are available that do not dry out, which is essential for long recordings as typical in sleep studies [112]. For electode density, in-ear EEG devices may use high-density montages to characterize spatial variations in voltage [26] or impedance [78] over the ear surface, or the ear canal [31], although most in-ear devices use 8 or fewer electrodes per ear [65]. Around-the-ear devices have mostly adopted a standard montage, with the cEEGrid [81] being the only ear-EEG device in our knowledge to provide an open-source plugin for visualizing topomaps of around-the-ear-EEG activity [113] for EEGLAB [114], an open-source EEG analysis and visualization toolbox that is frequently adopted by ear-EEG studies. Besides the cEEGrid montage, high-density around-the-ear montages have also been used to compare the signal quality of bipolar configurations for recording evoked EEG activity from around-the-ear [18].

B. Optical Sensing

Vital signals, including the arterial pulse, blood pressure, and blood oxygen, can be captured through optical approaches. Optical vital sign sensing techniques, such as PPG and pulse oximetry, utilize light to measure changes in blood volume and oxygen saturation, providing a non-invasive and continuous method for monitoring these critical parameters. Optical sensing methods, particularly PPG and pulse oximetry are widely used in in-ear sensors to monitor pulse and blood oxygen saturation (SpO_2) levels. The working principle of PPG involves emitting light from a source, typically a light-emitting diode, into the skin and measuring the amount of light that is absorbed by arteries. As blood pulses through these arteries, the varying blood volume changes the amount of light absorbed, which is then detected by a photodetector. This variation in light absorption corresponds to the pulse cycle, allowing the measurement of pulse rate [115], [116].

1) Photoplethysmography for Blood Oxygenation, Cardiovascular, and Respiratory Monitoring: For pulse oximetry, the PPG technique is extended by using two light sources with different wavelengths—usually red and infrared. Hemoglobin in the blood has different absorption rates to these wavelengths depending on whether it is oxygenated or deoxygenated. By comparing the absorption of the two wavelengths, the sensor can calculate the ratio of oxygenated to deoxygenated hemoglobin, providing an estimate of SpO_2. Fingertip sensors are widely used for SpO_2 but can be affected by peripheral vasoconstriction, especially in cold environments. While the ear provides a reliable site for SpO_2 measurement due to its stable blood flow, offering consistent readings. It has also been shown that in-ear SpO_2 response is faster than measurement from the finger. In a previous study, the known phenomena of time delay between central circulation and peripheral circulation has been measured with a mean delay of 12.3 s between the ear and finger when the subjects performed breath holds [117]. PPG data are further used to extract additional physiological information, such as heart rate variability (HRV) [118], pulse rate (PR) [116], blood pressure (combined with an air pump) [119], blood glucose [120], and SpO_2 [121]. Among them, HRV is a key indicator of autonomic nervous system activity, reflecting the balance between the sympathetic and parasympathetic branches of the autonomic nervous system. PR is a fundamental vital sign that provides insights into cardiovascular health, while blood pressure is a critical indicator of cardiovascular function. SpO_2 is a measure of the oxygen saturation level in the blood, reflecting the efficiency of oxygen delivery to tissues. These parameters are essential for monitoring cardiovascular health and stress levels, making PPG a valuable tool for health and wellness applications [1], [115], [122]. Beyond, one work led by Hammour and Mandic further expanded the principle of earable optical sensing to continuous, non-invasive blood glucose monitoring using a pulse oximeter, which is then combined with machine learning models to estimate blood glucose levels [120]. These parameters are essential for monitoring cardiovascular health and stress levels, making PPG a valuable tool for health and wellness applications [1], [115], [122].

Another main direction of research for ear PPG is respiration monitoring, which is critical for understanding and managing various health conditions, including respiratory diseases, cardiac ailments, and stress. The fluctuations of absorption of the two wavelengths are influenced by respiratory cycles, creating modulations in the PPG signal that can be analyzed to extract respiratory biomarkers such as respiratory rate (RR), breathing phases, and tidal volume [123], [124]. Apart from PPG, one study from Taniguchi and Nishikawa also investigated using infrared light to detect shape changes in the ear canal caused by breathing movements, offering a non-invasive and motion-resilient alternative for optical respiratory sensing [125].

However, PPG based optical sensing methods have limitations as well. The accuracy of PPG and SpO_2 measurements can be affected by factors such as skin tone [126], ambient light interference, and motion artifacts. Traditionally, vital signs including blood pressure requires cuff-based monitors for direct measurements, which are bulky and not suitable for continuous monitoring. Earable PPG alone is hard to make accurate estimate on BP. The common practice is to combine PPG with ECG at the ear to measure ECG-to-PPG pulse transit time (PTT) to provide better estimate of blood pressure non-invasively [127], [128], leveraging the ear's stable environment. Though ECG is not easily obtained in an integrated manner in the ear especially using a single ear ECG setup [43]. Additionally, in-ear placement poses unique challenges as the ear canal is a less stable measurement site compared to the fingertip or wrist, requiring sophisticated algorithms to mitigate motion artifacts and ensure reliable readings [119], [129].

2) Body Temperature: Infrared thermometry at the ear (tympanic membrane) is commonly used due to its proximity to the carotid artery and hypothalamus, making ear a viable location for estimating core body temperature. Previous studies demonstrate that tympanic thermometers can provide real-time, continuous temperature monitoring through infrared sensors integrated into earable devices [124], [130]. These devices, designed with customizable 3D printing techniques, aim to maintain a close fit in the ear canal, enhancing the core body temperature measurement accuracy. However, the accuracy of tympanic temperature measurements can be significantly affected by various factors. Cárdenas-García et al. [131] found that environmental conditions such as ambient temperature and humidity can introduce errors, as the ear canal is exposed to external influences that may not accurately represent the core body temperature. Additionally, changes in local blood flow and sensor positioning within the ear canal can cause discrepancies. Chaglla et al. [132] further illustrate this by showing how non-thermal equilibrium conditions can lead to thermal shock errors, necessitating a waiting period for the sensor to stabilize before accurate readings can be obtained. Addressing these issues is critical for developing reliable, non-invasive temperature sensing systems for practical and clinical use. Despite these challenges, ear-based core temperature sensing continues to evolve, leveraging advanced materials and designs to offer increasingly reliable and personalized monitoring solutions, particularly for clinical and at-home health applications. Advancements like graphene-inked infrared thermopile sensors have been developed to enhance accuracy by improving thermal conductivity and reducing IR light scattering. One study demonstrated that while these materials improve performance, continuous monitoring remains sensitive to positioning and user activity, which can affect the consistency of measurements [132].

C. Chemical Sensing

The in-ear sweat is a rich source of health-related analytes. Sweat, produced by eccrine glands, contains water, electrolytes, hormones, and metabolites, playing key roles in thermoregulation, stress response, and waste excretion [133]. In-ear sweat, though less studied, has significant potential for advancing our understanding of human physiology and health monitoring. The ear canal, with its unique environment and continuous exposure to external elements, produces perspiration that can provide critical insights into the body's biochemical state [134]. Given its proximity to the brain, in-ear sweat may also offer more precise indicators of neurological conditions and stress levels compared to other sweat sources. In addition, the proximity of the ear to the brain implies that in-ear sweat might provide a more precise indication of neurological disorders and stress levels compared to sweat from other parts of the body. Previous research has explored the use of optical sensing [120], and electrochemical sensing of biomarkers like glucose, lactate or sodium ion concentrations in the ear [13], [135], [136].

The metabolic profiles in the ear sweat can reflect the body's physiological and pathological state, making it a valuable, non-invasive medium for health monitoring [137], [138]. Among the metabolism related biomarkers, one of the most prominent biomarkers is lactate which is indicative of tissue oxygenation and metabolic stress. Elevated sweat-lactate levels can signal anaerobic metabolism, often associated with strenuous physical activity or certain medical conditions such as sepsis and ischemia [139]. Continuous monitoring of lactate can be particularly beneficial for athletes to optimize training and recovery, as well as for patients in critical care settings [140]. Glucose is another biomarker, which is crucial for monitoring metabolic health and managing diabetes. Sweat glucose levels, although lower than blood and ISF glucose levels, can be correlated with them and offer continuous, non-invasive monitoring for diabetic patients, aiding in better glycemic control and early detection of hypo- or hyperglycemic events [141]. Electrolytes, including sodium, potassium, and chloride, are vital for maintaining fluid balance, nerve function, and muscle contractions. Abnormal levels of these electrolytes in sweat can indicate dehydration, electrolyte imbalances, and disorders such as cystic fibrosis, which is characterized by elevated sweat chloride levels. Monitoring these electrolytes in real time can help manage conditions like dehydration and electrolyte imbalances, ensuring proper hydration and electrolyte replenishment, especially in athletes and individuals exposed to extreme environmental conditions [133]. Cortisol, the primary stress hormone, is another key biomarker found in sweat. Cortisol levels can provide insights into an individual's stress response, adrenal function, and circadian rhythms. Abnormal cortisol levels are associated with conditions such as Cushing's syndrome, Addison's disease, and chronic stress. Continuous monitoring of cortisol through sweat can aid in the management of these conditions by providing a non-invasive means to track hormonal fluctuations [142]. In addition, in-ear sweat contains a variety of biomarkers such as pH levels, proteins, peptides, lipids like cholesterol and squalene, and neuropeptides. These biomarkers can provide valuable diagnostic information for conditions such as skin disorders, infections, metabolic acidosis, immune responses, inflammation, hypercholesterolemia, oxidative stress, and neurological and psychological health [143], [144], [145], [146], [147].

Sweat-based lab analysis is commonly used for diagnosing pathophysiological states, but biosensing approaches are gaining attention for their real-time monitoring of metabolites and clinically relevant biomarkers [148]. The common mechanisms that are employed in this regard rely on optical, electrochemical, and mechanical-based biosensing to detect and quantify various biomarkers present in sweat, each offering unique advantages in terms of sensitivity, specificity, and integration [149], [150]. Electrochemical biosensors typically consist of electrodes made from advanced materials such as graphene, carbon nanotubes, and metal nanoparticles, which enhance the conductivity and surface area for analyte interaction [151]. Enzyme-based sensors for glucose and lactate, for example, use enzymes (glucose oxidase and lactate oxidase) that catalyze reactions with the target molecules to generate quantifiable electrical currents commensurate with their concentrations. In addition, measuring the potential difference across a selective membrane, ion-selective electrodes detect electrolytes such as sodium and potassium, therefore providing information on hydration state and electrolyte balance. So far, several such platforms have been reported representing an advancement of wearable health technology such as continuous monitoring of glucose, ketone, lactate and sodium. [13], [152], [153], [154] platforms, typically designed as flexible, skin-adherent patches, utilize advanced microfluidic and electrochemical sensing technologies to facilitate the analysis of the various analytes in sweat. Other than that, optical biosensing mechanisms, such as fluorescence, colorimetric, and chemiluminescence detection, complement electrochemical sensors by detecting changes in light properties due to biomarker interactions [155]. Mechanical biosensing, though less common, detects physical changes like pressure or volume associated with sweat production or specific biomarkers. Electrochemical biosensing is widely adopted for its high sensitivity and real-time measurement capabilities.

Several attempts have been made to detect health parameters in in-ear or proximally located locations. However, sweat-based biochemical monitoring studies are limited in specific ear locations, possibly due to the limitations of sweat harvesting technologies in the delicate sensory organ and the lower density of sweat glands. So far, several chemical biomarkers have been reported using earable sensing platforms. Gil et al. [135] have reported on an ear-worn device that can monitor sweat parameters, including pH, lactate, and cardiovascular parameters. The electrochemical techniques, amperometry, and potentiometry, were employed for monitoring the lactate and pH, respectively. Using this ear-worn device, the temporal profile has been successfully tested on the human subject for lactate and pH. Using a similar concept for lactate electrochemical monitoring, Xu et al. [13], have reported, an in-ear flexible sensing patch that can be installed on the earbuds. This multimodal sensor was coupled with the EEG for synchronous monitoring of brain activity and physiological lactate levels in human subjects.

Despite the enormous attention and advantages associated with in-ear sweat-based sensing such as non-invasiveness and continuous monitoring, various challenges are yet to be addressed to employ these strategies for comprehensive health monitoring. One of the intrinsic challenges is sweat production variability, which changes due to the change in physiological state, hydration status, and environmental conditions. Inter-individual sweat composition variability occurs evidently due to the diverse genetic setup and the weather conditions they live in, which can severely impact the consistency and reliability of the sensing data. As the ear locations are prone to contamination with dust, earwax, cosmetics, etc., these can interfere with the sensor's analytical performance. Comfort, fit, and user acceptance are other challenges, that may limit its use for monitoring longer intervals to obtain significant health information. Considering the potential of in-ear sweat in healthcare monitoring, future works would be directed toward its collection and the enrichment of the analytes for sensitive detection/monitoring of clinically important analytes.

D. Mechano-Acoustic Sensing

Mechano-acoustic sensing in wearable ear devices offers an innovative approach to detecting mechanical and acoustic vibrations using integrated accelerometers, gyroscopes, and microphones. These sensors capture physiological activities, such as occlusal force and tongue, jaw, and head movements, transforming these vibrations into meaningful data for health monitoring, human-computer interaction, and motion detection [156], [157], [158], [159]. In-ear devices are particularly effective at tracking head gestures and subtle movements, providing insights into posture, balance, and even facial expressions [158], [160], [161], [162].

Applications of mechano-acoustic sensing in earables hold significant promise across various domains. In health monitoring, earables have the potential to continuously track physiological signals such as respiratory patterns [163], [164], heart rate [165], [166] and gait analysis. Monitoring these signals holds significant potential for health applications, such as using in-ear mechano-acoustic sensors for gait tracking, which could indicate diseases like Parkinson's [167], and aid in rehabilitation for seniors to improve mobility and prevent falls [162]. Another area of application is tracking human activities such as tongue movement, chewing, head and body motion, and facial expressions, which can be utilized for human-computer interaction, including hands-free control via teeth gestures [168], as well as fitness assessments [169], [170]. For example, BreathPro demonstrates the capability of in-ear microphones to monitor breathing modes during running, employing a sophisticated signal processing pipeline and machine learning-based classification model to enhance accuracy that can be used for fitness assessment [171].

However, there are limitations and trade-offs with this technology. Mechano-acoustic sensors are sensitive to noise from external sources and non-relevant body movements, such as head shakes or environmental sounds, which can affect their accuracy in distinguishing between signal types. For example, when trying to detect gait movement, other motion such as chewing or talking will impact the accuracy to distinguish gait movement from other movement [159]. In addition, just like other motion-tracking wearables, earables fallshort in detecting broader human motion compared to leg and torso-worn wearable motion tracking devices [158], [172]. Still, this is a shortcoming to all motion detecting wearables. Wrist-worn devices, although great in detecting arm movement, tendto be inaccurate for gait tracking during slow movement, or when the subject uses a walking aid [173], [174]. Leg and torso-mounted wearables tend to do better for gait, but are not very useful when the subject is doing a stationary task such as driving and VR/AR [175]. Earables are no exception. Therefore, for future research, earables can be a crucial component of a multimodal system which combines data from earables with other body-worn sensors using advanced machine learning algorithms for improving activity monitoring [3], [159], [176]. This enables earables to contribute to both head-based and whole-body motion analysis, offering a more complete picture of a user's physical activity and physiological state [177], [178].

IV. Earable Stimulation

Earables can be used to deliver stimuli for neuromodulation using various modalities. In this section, we consider acoustic and electric (current) stimulation. Acoustic stimulation, delivered through sound waves or tones, can be used for therapeutic purposes, such as sound therapy in hyperacusis and tinnitus [180]. Transcutaneous current stimulation of the auricular branch of the vagus nerve at the ear has shown promise in managing conditions like epilepsy, depression, and chronic pain by modulating neural activity in the brainstem and higher brain regions. Other stimulation modalities have also been explored in literature, such as vibrotactile taVNS for improving working memory [181], or rigid ear canal inserts for providing biofeedback as pressure in bruxism [182].

A. Acoustic Stimulation

One of the key advantages of wearable in-ear technology is acoustic stimulation. The close proximity and occlusion of the ear canal enable both discreet hearing and noise cancellation. Beyond everyday use cases, audio stimulation can also target brain modulation. Research has demonstrated that acoustic stimulation can influence brain activity using methods like auditory steady-state response (ASSR) and auditory brainstem response (ABR). Furthermore, studies of various audio patterns have revealed potential therapeutic applications for users. In terms of applications, studies have demonstrated promising applications with acoustic stimulation such as tinnitus management, hearing health assessment, cognitive enhancement and relaxation, neuromodulation for pain and mood disorders, sleep induction and maintenance, and monitoring otoacoustic emissions. Tinnitus is a common symptom where the user hears a sound in the absence of an external source, often associated to damage in the inner ear or an underlying neurological issue. The intensity of tinnitus can vary from mild to severe with brief ringing that is easily masked and doesn't interfere with daily life, to a constant noise that disrupts sleep and affects various activities, respectively. Research has shown sound therapy utilizing acoustic stimuli such as white noise, pink noise, and other types of soothing sounds can potentially help mask the ringing from tinnitus providing relief to user [180]. Moreover, ABR is used for assessment of tinnitus [183].

B. Transcutaneous Auricular Vagus Nerve Stimulation

1) Anatomy and Brainstem Targets: Vagus nerve (VN) or the 10th cranial nerve is the longest cranial nerve in the body, forming 75% of the parasympathetic nervous system that mediates a state of "rest and digest" [184]. VN emerges bilaterally from the brainstem, connecting the brain to multiple body structures including the heart, lungs, and the gastrointestinal system (vagus is Latin for wandering). Just under the cranium (skull), VN sends off an auricular branch that receives somatosensory input from the auricle, innervating especially the cymba conchae [7], [9], [185], although the literature on auricle innervation in humans is sparse [186] and nerve locations could vary between subjects. As all nerve fibers in the auricle (including ABVN and other, non-vagal cranial and cervical nerve fibers) run only 1 mm to 1.5 mm deep between the skin and cartilage, the auricle provides easy access for transcutaneous electrical ABVN stimulation (taVNS) [187]. taVNS at the cymba conchae recruits sensory ABVN fibers that project directly to the nucleus of the solitary tract (NTS) in the brainstem, and higher order brain structures as evidenced by fMRI studies [188], [189]. A key target of taVNS is the locus coeruleus (LC), the main source of norepinephrine (NE) in the brain [190]. Although the mechanisms underlying taVNS's modulatory effects are not fully understood, the pathway for taVNS to affect a distant organ or pathology can be considered indirect, as sensory input through taVNS could either be directly modulating parasympathetic vagal efferents with downstream targets [9], or producing systemic (body-level) changes by influencing multiple neurotransmitters including gamma-aminobutyric acid (GABA) and Norepinephrine (NE) [191], similar to invasive vagus nerve stimulation (VNS) [66], [67].

2) Stimulation Optimization and Dosage: Stimulation parameters for taVNS can be set with the goal of delivering a target dose of electrical charge [192] at a stimulation intensity that could excite ABVN fibers [193]. Optimizable parameters include electrode size and stimulation site [194], and stimulation level as determined by current intensity (amplitude, mA), pulse width (μs), frequency (Hz), duty cycle (%, from pulse width and frequency), pulse-pause ratio (ON/OFF time, distinguishing tonic and phasic stimulation), pulse shape (monophasic or biphasic), and the total duration of taVNS [195]. Optimization of stimulation parameters has been attempted by recording fMRI, far-field vagus somatosensory evoked potentials (VSEPs), heart rate variability, and pupil diameter, but stimulation protocols are not yet standardized and can lead to mixed results. fMRI findings have provided support for stimulating the cymba conchae or the inner tragus [188], [189], [196], [197]. Earlier VSEP studies have compared pulse amplitudes [198] and frequencies near 1 Hz [199], whereas other VSEP and fMRI studies have run faster stimulation in the range 20 Hz with customized pulse amplitude (current intensity) between each subject's sensitivity and pain thresholds [9], [200]. If optimizing stimulation parameters using VSEP, it should be noted that muscular artifacts can confound

VSEP results [9], and appropriate artifact cancellation is needed to separate brainstem sources from artifactual responses [201]. Reports of taVNS affecting pupil diameter (as a biomarker of LC-NE activity) have been mixed [68], [202], [203], and a recent study comparing tonic (30s ON, 30s OFF) and phasic (1 s ON, 29 s OFF) stimulation protocols with all other parameters kept the same found transient pupil dilation for both tonic and phasic stimulation [204]. Similarly, inconsistencies have also been observed in taVNS's modulation of resting-state EEG band powers [67], [68] and P300 evoked potentials [192], [203], which may also be attributable to differences in stimulation protocols.

Summarizing variations in other taVNS stimulation parameters, a systematic review of 41 taVNS randomized clinical trials until July 2020 found interquartile range of stimulation current amplitudes to range from 0.2 mA to 5 mA, pulse width from 0.2 ms to 0.5 ms, and stimulation frequency from 10 Hz to 26 Hz. The choice of pulse width and frequency was seen to be consistent with implantable vagus nerve stimulation (VNS) protocols, which could be further optimized for ABVN as its fiber composition is different from the cervical vagus nerve targeted in implantable VNS [193]. The range of chosen current amplitudes across studies is attributable to possible differences in the stimulation electrode size, impedance of the skin-electrode interface, and procedure for determining the subjects' perceived sensory and pain thresholds [192]. Current-controlled stimulation (current clamp) is preferable over voltage-controlled stimulation to accommodate for variations in the electrode-skin interface impedance across subjects and hardware [192], [195].

3) Safety of taVNS: Overall, taVNS is considered safe, with the most frequently reported adverse effects being mild and transient ear pain, headache, and tingling [205]. Additionally, there is evidence that taVNS can be self-administered with remote supervision as needed [206]. However, accurate dosage for taVNS is currently unknown and raises potential safety concerns, as invasive VNS studies have reported opposing neuromodulatory effects with changing dosage, for instance, in protocols targeting inflammation [193]. Furthermore, as effects of stimulation seen in a clinical population may not carry over to a healthy population, multimodal sensing and analysis is crucial for monitoring downstream effects of taVNS, for instance, on multimodal physiological markers assessing stroke volume and contractility in a taVNS study targeting stress [207].

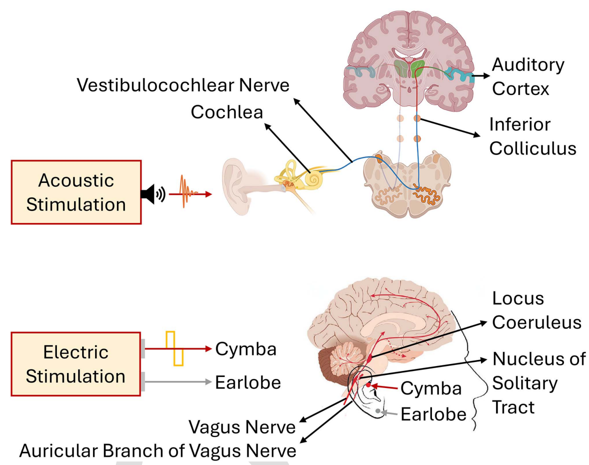

Fig. 5. Acoustic and electric stimulation modalities targeting the vestibulocochlear nerve and the auricular branch of vagus nerve (ABVN) respectively, with downstream targets. Left: stimulation modalities with time domain representation of illustrative stimulation patterns: a burst for sound, and a biphasic current pulse. Actual stimulation patterns used vary across studies and pathology. Right: pathway of the stimuli to subcortical and cortical targets. Sound stimulation travels through multiple nuclei including the inferior colliculus (IC) before reaching the auditory cortex in the temporal lobe [179]. ABVN projects to the neucleus tractus solitarius (NTS), with downstream targets including locus coeruleus (LC) and other brain regions [67]. Sources of anatomical drawings: auditory pathway © 2022 Jacxsens, De Pauw, Cardon, van der Wal, Jacquemin, Gilles, Michiels, Van Rompaey, Lammers and De Hertogh [179], ABVN pathway © 2021 Sharon et al. [67].

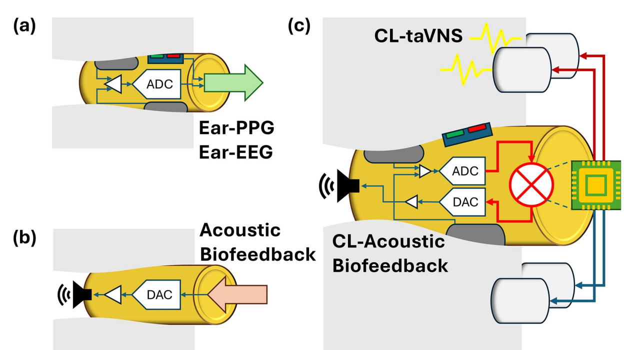

Fig. 6. Schematic overview of the earable biofeedback system. (a) Sensing system showing electrodes, amplifier, and ADC for in-ear EEG acquisition, combined with an integrated PPG sensor. (b) Auditory stimulation system consisting of a digital to analog converter (DAC) and speaker driver (taVNS not shown), (c) Biofeedback earable combining the sensing and stimulation pipelines from (a) and (b) through a modulator which could be realized on an integrated circuit for controlling the biofeedback. taVNS stimulation electrodes are also shown, targeting cymba concha on the top with earlobe reference on bottom (anatomical features not visualized).

V. Earable System Integration

A. Sensing Pipeline

The signal flow in a multimodal earable system begins at the sensors, where physiological data is detected. ExG signals, being typically weak, require immediate amplification by an analog front-end, which could include amplifiers and analog-to-digital converters as visualized in Fig. 6(a). For chemical sensors, a potentiostat controls the sensor operation and measures the resultant signals. Integrated digital sensors, like those for PPG and temperature, provide direct digital output through standard serial interfaces such as serial peripheral interface (SPI), inter-integrated circuit (I2C), or universal asynchronous receiver-transmitter (UART). All these signals, whether analog or digital, are then processed by a computational unit. Preprocessing or conditioning of signals, such as filtering and noise reduction, can be carried out either via dedicated hardware or within the computational unit for real-time applications. Alternatively, more extensive processing can be performed on a host machine via a wireless interface, leveraging greater computational power.

B. Stimulation Pipeline

The stimulation pipeline can be thought of as the sensing pipeline, but in reverse. To consider the case of acoustic stimulation, sound is delivered by a speaker, driven by a digital-to-analog converter and amplifier for driving the speaker as shown in Fig. 6(b). Current stimulation (not visualized) is conceptually analogous, with electrodes to deliver the current impulses, driven by DACs and amplifiers. Design considerations for DACs and amplifiers will be different for audio or current stimulation.

C. Multimodal Synchronization

Ear-EEG devices typically record from one or more channels from one or both ears, and the ear-EEG streams may further be combined with other data streams from scalp-EEG for validation [105] Data synchronization is crucial for integrative analysis, and a popular open-source software library that address the synchronization problem is Lab Streaming Layer (LSL) [208]. LSL ensures that all incoming data, regardless of the source, are time-stamped with high precision and synchronized across different data streams. As an illustration, a study evaluating the synchronization of audio streaming from a hearing aid development platform, and a separate ear-EEG stream from a cEEGrid Smarting acquisition could be synchronized within a jitter (standard deviation of latencies across trials) of 3 ms using LSL, making it suitable for developing closed-loop audio and ear-EEG processing systems [209], [210]. However, it is important to acknowledge that the complexities of LSL still require careful attention to timing tests of experimental setups, especially for time-sensitive analysis. For more accurate synchronization between streams, system-specific latency and jitter tests such as clock skew and network delay checks are recommended to verify proper synchronization.

D. Mechanical Shell Design

The mechanical design of ear sensor shells plays a crucial role in the effectiveness and comfort of earable devices, particularly when it comes to embedding sensors for the modalities such as ExG, PPG, temperature monitoring, and motion detection. These shells can be broadly categorized into subject-customized and generic designs, each with distinct considerations for accommodating the necessary electronics, including circuit boards, radio frequency (RF) components, and batteries.

1) Subject-Customized Earpiece: These are tailored specifically to an individual's ear anatomy. The process begins with a scan of the user's ear canal, capturing the unique contours and dimensions. Using this data, a 3D-printed mechanical shell is fabricated, designed to fit the ear for one particular subject [22], [51], [93] This customized approach is particularly beneficial for ear-ExG, where precise electrode placement and stable contact with the skin are essential for high-quality signal acquisition. The snug fit minimizes movement artifacts, enhances comfort, and allows for the reliable long-term monitoring of neural activity. Additionally, customized shells can accommodate other sensors such as PPG sensors for heart rate and oxygen saturation, which benefit from stable contact with the richly vascularized areas of the ear. Temperature sensors can be integrated to measure core body temperature from within the ear canal, taking advantage of the shell's close fit and thermal insulation properties.

2) Generic Earpiece: These, on the other hand, are not tailored to any specific individual but are instead created to fit a broad range of users. These designs typically utilize flexible or adjustable components to accommodate various ear shapes and sizes, making them more versatile and cost-effective for mass production. Generic earpieces may adopt an earbud-like structure [13], [25], [89], [91], [211] that includes multiple embedded sensors, such as accelerometers for motion detection, PPG sensors, and temperature sensors. While generic designs may not offer the precise fit of customized shells, advancements in material science and ergonomic design have allowed these shells to achieve a balance between usability, comfort, and performance.

3) Printed Circuit Board (PCB): When considering the integration of electronics, polyimide flexible printed circuit boards (PCB) are usually employed to conform to the unique shape of the ear, ensuring that the electronic components are seamlessly embedded without compromising the fit or comfort. Flexible PCBs are advantageous in these designs as they can be molded to the intricate curves of the ear, providing reliable connections between sensors, amplifiers, and other electronic components. The placement of RF components, such as Bluetooth transmitters, is carefully considered to minimize interference and preserve signal quality, often being positioned in areas of the shell that are less likely to experience attenuation due to proximity to skin or bone.

Battery placement is another critical factor, the battery is typically positioned in a location that balances weight distribution and thermal management, often in the outer portion of the ear where heat dissipation is more effective, thus preventing discomfort during prolonged use. In both customized and generic designs, the careful integration of electronics is essential to maintain the overall functionality, comfort, and performance of the earable device. The design must account for the unique thermal, mechanical, and electronic challenges posed by the small, complex environment of the ear, ensuring that all components work together harmoniously to deliver accurate, reliable health monitoring. Lastly, sound hole structures are usually included in either customized or generic earpiece to preserve the fundamental acoustic transmission functionality of the earable system.

VI. Closing the Loop

This section motivates building a closed-loop biofeedback system by combining the sensing and stimulation systems into one earable, as visualized in Fig. 6(c). Here we focus on some key ingredients that could help optimize the biofeedback's control

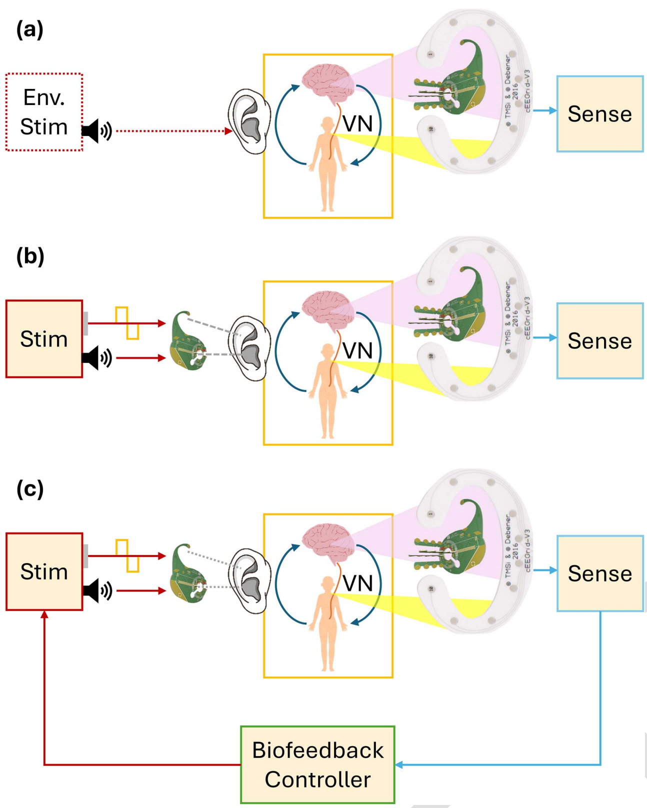

Fig. 7. Various configurations for combining sensing, stimulation, and biofeedback in an earable. Brain and body coupling visualized here through cervical vagus nerve (VN) originating from the brainstem. (a) Earable as a monitoring system in the user's natural acoustic environment (Env.), with no additional stimulation provided by the earable. Monitoring targets include brain activity as projected to in-ear and around-the-ear electrodes (as a pink beam), and cervical vagus nerve activity projecting to lower around-the-ear electrodes (as a yellow beam), motivated by results from [212]. (b) Earable with open-loop stimulation and continuous monitoring. Stimuli include electrical (taVNS) and acoustic stimulation to the ear. (c) Closing the loop through a biofeedback controller. Visualized ear-EEG devices are croc V2 [31] (©2023 IEEE), and cEEGrid [17].

policy to be used for adapting the stimulation given incoming sensory information.

A. Continuous Monitoring With Environmental Stimuli

Given the potential of earables to collect long durations of unlabelled data, and analysis methods to assess changes in a subject's state, for example, in ear-EEG sleep studies [46], [213], we first consider earables for continuous assessment of biomarkers and physiomarkers in the presence of only environmental stimuli, that is, where no stimulation is applied by the device, as shown in Fig. 7(a).

In a series of three studies, Hölle et al. have demonstrated that ear-EEG can be recorded beyond-the-lab using a wearable setup [214], [215], [216]. These studies measured ERPs either in response to auditory oddball stimuli [214] or naturalistic sounds [215], [216], delivered either in a lab, office, cafeteria, or home-office environment. Larger P300 ERP responses to target stimuli were seen, compared to standard stimuli, but naturalistic sounds did not evoke strong ERPs [216]. For oddball stimuli, the test tones were not deemed disruptive by subjects performing office work, but ear-EEG responses to naturally occurring sounds that are ecologically meaningful to the participants, such as their names or ringtones, could also be considered [214].

To enable real-life recording of synchronized EEG with concurrent soundscapes: AFEx (Audio Feature Extraction Framework) and Record-a. AFEx enables real-time audio capture, privacy-preserving feature extraction from the audio, and LSL streaming of three features: power spectral density, root-mean square power, and sound onsets. Audio can be captured using wired microphones, which could be worn binaurally behind the ears (to not occlude environmental sounds from entering the ear canals), connected to a smartphone running AFEx. Simultanseously, ear-EEG is recorded and streamed using a wearable data acquisition device. The smartphone then runs Record-a for synchronized recording (using LSL) of the incoming streams carrying audio features and ear-EEG. Although new audio features could be implemented, for instance, as extracted by models of the auditory periphery [217], [218], for tuning feature extraction for pathologies such as hearing impairment. Any new features, however, will have to be evaluated for privacy [215].

B. Open-Loop Stimulation

It may seem trivial to first deploy a biofeedback earable without the feedback, that is, in open-loop, but open-loop stimulation can have beneficial outcomes. This configuration is visualized in Fig. 7(b).

As evidence of potential benefits of open-loop stimulation, we summarize accumulating findings from the Gamma ENtrainment Using Sensory Stimuli (GENUS) program. Sensory stimulation aimed at entraining gamma oscillations in a mouse model of Alzheimer's disease (5XFAD) has shown a reduction in amyloid plaques in the visual cortex when using 40 Hz light stimulation [219], in the auditory cortex and hippocampus when using 40 Hz audio stimulation (1 ms long, 10 kHz tones), and more widespread reduction of plaques in the neocortex when audio and visual stimulation is combined with aligned onsets [220]. Intriguingly, the same rate of 40 Hz was found to be the most effective for both modalities, individually and when delivered together. The choice of 40 Hz was motivated by noting that reduced gamma power is reported for Alzheimer's mouse models with a clearance mechanism identified as 40 Hz stimulation recruiting the glymphatic system, critical for removing metabolic waste (and plaque) from the brain [221]. 40 Hz sensory stimulation has also been applied to mouse models of neurodegeneration, with 40 Hz visual [222], or 40 Hz vibrotactile [223] stimulation entraining gamma activity and reducing pathology. Finally, a feasibility pilot in humans with mild Alzheimer's has shown positive outcomes for 40 Hz audiovisual stimulation [224]. Therefore, open-loop stimulation across multiple sensory modalities can activate pathways that may still be beneficial in certain pathologies and target brain areas.

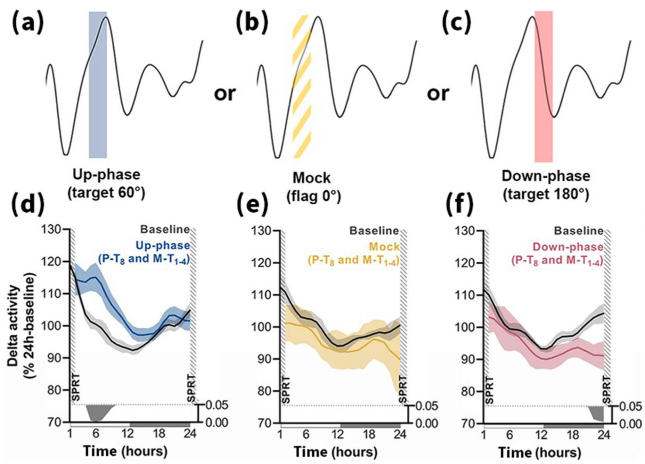

Fig. 8. Closed-loop acoustic/auditory stimulation (CLAS) concept and its effects on slow-wave sleep from a validation study in an animal model (rat) by Moreira et al. [225]. Top: Acoustic stimulation's phase with respect to ongoing slow oscillations in slow-wave sleep. Stimulation targeted either the (a) up-phase, (c) down-phase, or (b) no stimulation was provided (mock). Bottom: Grand-averaged time course of delta activity (0.5 Hz to 4 Hz) over 12 days of training with CLAS, where (d) targeting up-phase enhanced delta activity, (e) no stimulation (mock) had no significant effect, and, (f) targeting down-phase decreased delta activity. Gray shadows below plots show significant time-points (multiple t-tests, Holm–Sidak corrected). Time: 0–12 correspond to light, and 12–24 are dark periods. PT: Pre-Training (8 days), MT: Motor-Training (4 days). Rat subjects were trained to perform a single-pellet reaching task (SPRT), timing shown. ©2021, Moreira et al. [225].

C. Earables for Closed-Loop Biofeedback

As depicted in Fig. 7(c), earables can be used to deliver closed-loop acoustic and current stimulation, where sensory monitoring is used to control stimulation parameters and dosage, thus closing the loop. In this section, we provide examples of stimulation strategies that have shown promising results using acoustic stimulation or taVNS in the biofeedback literature, positioning them for follow-up translational work using earables to provide the biofeedback.

1) Closed-Loop Acoustic Stimulation: Sleep and stress management can have an important impact on improving people's quality of life. With increasing urbanization, there is more exposure to external noise, and such ambient sounds typically have an adverse effect on sleep. Although barriers such as earmuffs can help reduce disturbance from external noise, studies have demonstrated that various forms of acoustic stimulation can also help mask the undesirable sounds [226]. Acoustic stimulation also has the potential to alleviate stress, promoting relaxation, utilizing calming soundscapes to lower anxiety levels and encourage relaxation [227]. Next, we review supporting evidence for one particular strategy for closed-loop acoustic stimulation and its impact on enhancing slow wave sleep.

Closed-loop Auditory (Acoustic) Stimulation (CLAS) is to play acoustic stimuli, such as brief 1/f pink noise bursts, in-phase with ongoing slow oscillations (0.1 Hz–1 Hz) observed during non-rapid eye movement (NREM) sleep.This stimulation strategy is visualized in Fig. 8, reproduced from a recent validation study in an animal model [225]. For human subjects, a recent review of CLAS by Esfahani et al. [228] summarizes stimulation parameters and results from 14 CLAS studies from 2013 to 2022, all providing encouraging evidence for increasing the amplitude of slow oscillations, and a potential for improving memory consolidation, although reports have been mixed for memory effects, possibly confounded by stimulation parameters, target group, and off-target stimulation applied to delta wave activity (smaller amplitude local events) instead of slow oscillations (larger amplitude global slow waves) [229].

2) Earables for Closed-Loop taVNS: Given the accessibility of ABVN for electrical stimulation from the auricle, and the feasibility of ear-EEG for measuring attention biomarkers such as alpha power, merging taVNS and ear-EEG for closed-loop (CL) attention modulation of taVNS stimulation parameters using simultaneous ear-EEG has been suggested previously [123]. The form factor of in-ear EEG devices could provide access to taVNS stimulation sites including the conchae (cymba and cavum), tragus, and the ear canal, while around-the-ear devices such as the cEEGrid could be adapted for tragus stimulation.

CL-taVNS systems could support phasic taVNS protocols by time-multiplexing ear-EEG recording and taVNS to avoid stimulation artifacts from corrupting ear-EEG. For tonic protocols, stimulation artifact reduction could be achieved using real-time compatible Generalized Eigenmode Decomposition (GED) [230], or device constraints permitting, a separate stimulation reference channel could be added behind the earlobe for artifact removal [231].

The optimal EEG biomarker of LC activity as mediated by taVNS can be expected to evolve as the mechanistic understanding of taVNS advances. For instance, using alpha power as a biomarker of LC activity as suggested previously [66] was not reproducible in a replication study [68], but alpha activity could still be modulated by taVNS during cognitive tasks [191], [232]. In addition to alpha power, ear-EEG devices have been validated for recording other brain responses including the P300, and extending ear-EEG to multimodal earables could additionally provide ear-ECG, ear-PPG, electrochemical sensing, and derivative biomarkers such as heart rate [233], HRV [118], and breathing phase [123]. Breathing phase could especially be relevant for protocols aligning taVNS stimulation with the expiration phase [234], or their invasive VNS counterparts [235].

D. Earables With On- and Off-Target Nerve Activity Monitoring

Earables also harbor the possibility of measuring neural biomarkers of vagus nerve activity. Cervical electroneurography is a recent non-invasive method for recording cervical VN activity from the neck using an adhesive array of Ag/AgCl electrodes [212]. Two of the rostrally placed electrodes of the reported electrode array appear visibly close to the L5, L6, R5, and R6 electrodes of around-the-ear cEEGrid devices, suggesting that cEEGrids could be evaluated for non-invasive monitoring of cervical VN activity as a downstream target for acoustic/taVNS biofeedback. Non-invasive monitoring of ABVN activity has also been attempted using in-ear electrodes to assess the autonomic nervous system's response under physiological stressors (cold face test and cold pressor test) [236], but given the preliminary stage of in-ear ABVN monitoring, follow-up source localization studies can eliminate possible confounds through in-silico modeling [237], [238], or minimally-invasive recording such as microneurography to measure simultaneously from the cervical VN [206] and other, off-target nerves in the auricle, such as greater auricular nerve in the ear lobe [239].

Regardless of the in-ear electrodes picking ABVN activity or sympathetic efferents, the possibility of accessing a neural biomarker from the ear could help monitor the efficacy of biofeedback, analogous to using evoked compound action potentials (eCAPs) measured from cervical VN for dosing VNS [240]. To summarize, earables combining stimulation with monitoring through ear-ExG, chemical sensing, and potentially VN activity, could become a candidate platform for optimizing biofeedback dosage with simultaneous stimulation and monitoring of downstream effects through the same earable.

VII. Conclusion

The ear offers a rich source of brain and body biosignals that can be unobtrusively tapped as a highly versatile and powerful means for continuous cognitive and metabolic health monitoring, and further combined with equally unobtrusive stimulation applied to the ear for biofeedback and neuromodulation therapy. The ability of earables to integrate stimulation mechanisms with sensing capability provides a non-invasive, comfortable, and socially acceptable way to deliver therapeutic interventions. This integration not only enhances the functionality of earable technology but also opens new avenues for personalized health management and neurotherapy, leveraging the ear's unique anatomical and neural connections for effective and unobtrusive stimulation. Follow-up studies are needed to establish the longer-term outcomes and optimization of stimulation control based on fused biosignals, but the potential of earables for personalizing bioelectronic therapeutics with continuous monitoring may lead to engineered naturalistic remediation of drug-resistant pathologies.

Acknowledgment

The authors would like to thank Virginia R. de Sa, Fiza Singh, Lara M. Rangel, Andrea Chiba, Benjamin L. Smarr, Shlomo Dubnov, Vikrant Jaltare, M. Florencia Assaneo, Shihab Shamma, John R. Iversen, Dick Lyon, Simon Carlile, Jason Mikiel-Hunter, Tzzy-Ping Jung, and attendees of the 2021 Telluride Neuromorphic Cognition Engineering Workshop, Simula Summer School in Computational Physiology, Australian Hearing Hub's Signal Processing for Hearing – Lecture Series, and the van Vreeswijk Theoretical Neuroscience Seminars for helpful discussions and insights that directly and indirectly shaped our outlook on neuromodulation.

References

[1] V. Goverdovsky et al., "Hearables: Multimodal physiological in-ear sensing," *Sci. Rep.*, vol. 7, no. 1, Jul. 2017, Art. no. 6948.

[2] D. Mandic et al., "In your ear: A multimodal hearables device for the assessment of the state of body and mind," *IEEE Pulse*, vol. 14, no. 6, pp. 17–23, Nov./Dec. 2023.

[3] T. Röddiger et al., "Sensing with earables: A systematic literature review and taxonomy of phenomena," in *Proc. ACM Interact. Mobile Wearable Ubiquitous Technol.*, Sep. 2022, vol. 6, pp. 1–57.

[4] J.-Y. Choi et al., "Health-related indicators measured using earable devices: Systematic review," *JMIR mHealth uHealth*, vol. 10, no. 11, Nov. 2022, Art. no. e36696.

[5] M. Masè et al., "Hearables: New perspectives and pitfalls of in-ear devices for physiological monitoring. A scoping review," *Front. Physiol.*, vol. 11, Oct. 2020, Art. no. 568886.

[6] R. S. Tyler et al., "An exploratory study of bimodal electro-aural stimulation through the ear canals for tinnitus," *Amer. J. Audiol.*, vol. 33, no. 2, pp. 455–464, Jun. 2024.

[7] B. Dabiri et al., "High-resolution episcopic imaging for visualization of dermal arteries and nerves of the auricular cymba conchae in humans," *Front. Neuroanat.*, vol. 14, May 2020, Art. no. 22.

[8] P. Bermejo et al., "Innervation of the human cavum conchae and auditory canal: Anatomical basis for transcutaneous auricular nerve stimulation," *BioMed Res. Int.*, vol. 2017, no. 1, 2017, Art. no. 7830919.

[9] M. F. Butt et al., "The anatomical basis for transcutaneous auricular vagus nerve stimulation," *J. Anatomy*, vol. 236, no. 4, pp. 588–611, 2020.

[10] V. Hládek et al., "Real-time estimation of horizontal gaze angle by saccade integration using in-ear electrooculography," *PLoS One*, vol. 13, no. 1, Jan. 2018, Art. no. e0190420.

[11] A. Favre-Félix et al., "Absolute eye gaze estimation with biosensors in hearing aids," *Front. Neurosci.*, vol. 13, Dec. 2019, Art. no. 1294.

[12] M. A. Skoglund et al., "Comparing in-ear EOG for eye-movement estimation with eye-tracking: Accuracy, calibration, and speech comprehension," *Front. Neurosci.*, vol. 16, Jun. 2022, Art. no. 873201.

[13] Y. Xu et al., "In-ear integrated sensor array for the continuous monitoring of brain activity and of lactate in sweat," *Nat. Biomed. Eng.*, vol. 7, no. 10, pp. 1307–1320, Oct. 2023.

[14] S. Park et al., "Systematic investigation of optimal electrode positions and re-referencing strategies on ear biosignals," *Int. J. Hum.–Comput. Interact.*, pp. 1–20, Feb. 2024.

[15] D. Looney et al., "The in-the-ear recording concept: User-centered and wearable brain monitoring," *IEEE Pulse*, vol. 3, no. 6, pp. 32–42, Nov. 2012.

[16] K. B. Mikkelsen et al., "EEG recorded from the ear: Characterizing the Ear-EEG method," *Front. Neurosci.*, vol. 9, Nov. 2015, Art. no. 438.

[17] S. Debener et al., "Unobtrusive ambulatory EEG using a smartphone and flexible printed electrodes around the ear," *Sci. Rep.*, vol. 5, no. 1, Nov. 2015, Art. no. 16743.

[18] A. Meiser et al., "High-density ear-EEG for understanding ear-centered EEG," *J. Neural Eng.*, vol. 21, no. 1, Jan. 2024, Art. no. 016001.

[19] S. L. Kappel et al., "Ear-EEG forward models: Improved head-models for Ear-EEG," *Front. Neurosci.*, vol. 13, Sep. 2019, Art. no. 943.

[20] M. C. Yarici et al., "Ear-EEG sensitivity modeling for neural sources and ocular artifacts," *Front. Neurosci.*, vol. 16, Jan. 2023, Art. no. 997377.

[21] "Sleep in orbit," 2023. Accessed: Aug. 30, 2024. [Online]. Available: ece.au.dk. https://ece.au.dk/forskning/forskningscentre/center-for-ear-eeg/projects/sleep-in-orbit

[22] D. Looney et al., "An in-the-ear platform for recording electroencephalogram," in *Proc. 2011 Annu. Int. Conf. IEEE Eng. Med. Biol. Soc.*, Aug. 2011, pp. 6882–6885.

[23] M. G. Bleichner et al., "Exploring miniaturized EEG electrodes for brain-computer interfaces. an EEG you do not see?," *Physiol. Rep.*, vol. 3, no. 4, 2015, Art. no. e12362.

[24] L. Fiedler et al., "Ear-EEG allows extraction of neural responses in challenging listening scenarios — A future technology for hearing aids?," in *Proc. 38th Annu. Int. Conf. IEEE Eng. Med. Biol. Soc.*, Aug. 2016, pp. 5697–5700.

[25] V. Goverdovsky et al., "In-ear EEG from viscoelastic generic earpieces: Robust and unobtrusive 24/7 monitoring," *IEEE Sensors J.*, vol. 16, no. 1, pp. 271–277, Jan. 2016.

[26] S. L. Kappel and P. Kidmose, "High-density ear-EEG," in *Proc. 39th Annu. Int. Conf. IEEE Eng. Med. Biol. Soc.*, Jul. 2017, pp. 2394–2397.

[27] S. L. Kappel et al., "Dry-contact electrode ear-EEG," *IEEE Trans. Biomed. Eng.*, vol. 66, no. 1, pp. 150–158, Jan. 2019.

[28] R. Kaveh et al., "A wireless, multielectrode, user-generic ear EEG recording system," in *Proc. 2019 IEEE Biomed. Circuits Syst. Conf.*, Oct. 2019, pp. 1–4.

[29] A. Paul et al., "Integrated in-ear device for auditory health assessment," in *Proc. 41st Annu. Int. Conf. IEEE Eng. Med. Biol. Soc.*, Jul. 2019, pp. 56–59.

[30] B. Tracey et al., "A novel, wearable, in-ear EEG technology to assess sleep and daytime sleepiness," *Sleep Medicine*, vol. 115, p. S205, Feb. 2024.

[31] M. S. Lee et al., "Scalable anatomically-tunable fully in-ear dry-electrode array for user-generic unobtrusive electrophysiology," in *Proc. 45th Annu. Int. Conf. IEEE Eng. Med. Biol. Soc.*, Jul. 2023, pp. 1–4.

[32] Z. Wang et al., "Conformal in-ear bioelectronics for visual and auditory brain-computer interfaces," *Nat. Commun.*, vol. 14, no. 1, Jul. 2023, Art. no. 4213.

[33] H. Zhao et al., "Optimization of ear electrodes for SSVEP-based BCI," *J. Neural Eng.*, vol. 20, no. 4, Jul. 2023, Art. no. 046011.

[34] M. Zeydabadinezhad et al., "A personalized earbud for non-invasive long-term EEG monitoring," *J. Neural Eng.*, vol. 21, no. 2, Apr. 2024, Art. no. 026026.

[35] X. Zhou et al., "A wearable ear-EEG recording system based on dry-contact active electrodes," in *Proc. IEEE Symp. VLSI Circuits*, Jun. 2016, pp. 1–2.

[36] J. Lee et al., "A 0.8-V 82.9-muW in-ear BCI controller IC with 8.8 PEF EEG instrumentation amplifier and wireless BAN transceiver," *IEEE J. Solid-State Circuits*, vol. 54, no. 4, pp. 1185–1195, Apr. 2019.

[37] A. Paul et al., "Neural recording analog front-end noise reduction with digital correlated double sampling," in *Proc. 2022 IEEE Biomed. Circuits Syst. Conf.*, Oct. 2022, pp. 149–152.

[38] A. Paul et al., "A versatile in-ear biosensing system and body-area network for unobtrusive continuous health monitoring," *IEEE Trans. Biomed. Circuits Syst.*, vol. 17, no. 3, pp. 483–494, Jun. 2023.

[39] R. Kaveh et al., "Wireless ear EEG to monitor drowsiness," *Nat. Commun.*, vol. 15, no. 1, Aug. 2024, Art. no. 6520.

[40] A. Meiser and M. G. Bleichner, "Ear-EEG compares well to cap-EEG in recording auditory ERPs: A quantification of signal loss," *J. Neural Eng.*, vol. 19, no. 2, Apr. 2022, Art. no. 026042.

[41] G. Correia et al., "Brain wearables: Validation toolkit for ear-level EEG sensors," *Sensors (Basel, Switzerland)*, vol. 24, no. 4, Feb. 2024, Art. no. 1226.

[42] W. von Rosenberg et al., "Hearables: Feasibility of recording cardiac rhythms from head and in-ear locations," *Roy. Soc. Open Sci.*, vol. 4, no. 11, Nov. 2017, Art. no. 171214.

[43] M. Yarici et al., "Hearables: Feasibility of recording cardiac rhythms from single in-ear locations," *Roy. Soc. Open Sci.*, vol. 11, no. 1, Jan. 2024, Art. no. 221620.

[44] A. Meiser et al., "The sensitivity of Ear-EEG: Evaluating the source-sensor relationship using forward modeling," *Brain Topogr.*, vol. 33, no. 6, pp. 665–676, Nov. 2020.

[45] T. W. Kjaer et al., "Repeated automatic sleep scoring based on ear-EEG is a valuable alternative to manually scored polysomnography," *PLoS Digit. Health*, vol. 1, no. 10, Oct. 2022, Art. no. e0000134.

[46] K. Borup et al., "Automatic sleep scoring using patient-specific ensemble models and knowledge distillation for ear-EEG data," *Biomed. Signal Process. Control*, vol. 81, Mar. 2023, Art. no. 104496.

[47] G. Hammour et al., "Hearables: Automatic sleep scoring from single-channel Ear-EEG in older adults," in *Proc. 45th Annu. Int. Conf. IEEE Eng. Med. Biol. Soc.*, Jul. 2023, pp. 1–4.

[48] H. Phan et al., "L-SeqSleepNet: Whole-cycle long sequence modeling for automatic sleep staging," *IEEE J. Biomed. Health Informat.*, vol. 27, no. 10, pp. 4748–4757, Oct. 2023.

[49] N. Pham et al., "Detection of microsleep events with a behind-the-ear wearable system," *IEEE Trans. Mobile Comput.*, vol. 22, no. 2, pp. 841–857, Feb. 2023.

[50] S. Waters et al., "Domain adaptation using large scale databases for sleep staging from a novel in-ear sensor," *Res. Square*, Feb. 2024.

[51] I. C. Zibrandtsen et al., "Ear-EEG detects ictal and interictal abnormalities in focal and generalized epilepsy–A comparison with scalp EEG monitoring," *Clin. Neuriophysiol.*, vol. 128, no. 12, pp. 2454–2461, Dec. 2017.

[52] C. S. Musaeus et al., "Subclinical epileptiform discharges in alzheimer's disease are associated with increased hippocampal blood flow," *Alzheimer's Res. Ther.*, vol. 16, no. 1, Apr. 2024, Art. no. 80.

[53] M. Joyner et al., "Using a standalone ear-EEG device for focal-onset seizure detection," *Bioelectron. Med.*, vol. 10, no. 1, Feb. 2024, Art. no. 4.

[54] N. Kaongoen et al., "Speech-imagery-based brain–computer interface system using ear-EEG," *J. Neural Eng.*, vol. 18, no. 1, Feb. 2021, Art. no. 016023.

[55] X. Li et al., "The classification of SSVEP-BCI based on ear-EEG via RandOm convolutional KErnel transform with morlet wavelet," *Discover Appl. Sci.*, vol. 6, no. 4, Mar. 2024, Art. no. 149.

[56] P. Israsena and S. Pan-Ngum, "A CNN-Based deep learning approach for SSVEP detection targeting binaural Ear-EEG," *Front. Comput. Neurosci.*, vol. 16, May 2022, Art. no. 868642.

[57] Y.-T. Wang et al., "Developing an online steady-state visual evoked potential-based brain-computer interface system using EarEEG," in *Proc. 37th Annu. Int. Conf. IEEE Eng. Med. Biol. Soc.*, Aug. 2015, pp. 2271–2274.

[58] Y.-T. Wang et al., "An online brain-computer interface based on SSVEPs measured from non-hair-bearing areas," *IEEE Trans. Neural Syst. Rehabil. Eng.*, vol. 25, no. 1, pp. 14–21, Jan. 2017.

[59] C. B. Christensen et al., "Chirp-evoked auditory steady-state response: The effect of repetition rate," *IEEE Trans. Biomed. Eng.*, vol. 69, no. 2, pp. 689–699, Feb. 2022.

[60] L. Fiedler et al., "Single-channel in-ear-EEG detects the focus of auditory attention to concurrent tone streams and mixed speech," *J. Neural Eng.*, vol. 14, no. 3, Apr. 2017, Art. no. 036020.

[61] M. Thornton et al., "Decoding of selective attention to speech from Ear-EEG recordings," Nov. 2024, *arXiv:2401.05187*.

[62] S. Geirnaert et al., "Fast, accurate, unsupervised, and time-adaptive eeg-based auditory attention decoding for neuro-steered hearing devices," in *Brain-Computer Interface Research*, C. Guger et al. Eds. Berlin, Heidelberg, Germany: Springer, 2024, pp. 29–40.

[63] C. K. H. Ne et al., "Hearables, in-ear sensing devices for bio-signal acquisition: A narrative review," *Expert Rev. Med. Devices*, vol. 18, no. sup 1, pp. 95–128, Dec. 2021.

[64] N. Kaongoen et al., "The future of wearable EEG: A review of ear-EEG technology and its applications," *J. Neural Eng.*, vol. 20, no. 5, Oct. 2023, Art. no. 051002.

[65] J. Y. Juez et al., "Ear-EEG devices for the assessment of brain activity: A review," *IEEE Sensors J.*, vol. 24, no. 20, pp. 31606–31623, Oct. 2024.

[66] P. Ruhnau and T. Zaehle, "Transcranial auricular vagus nerve stimulation (taVNS) and Ear-EEG: Potential for closed-loop portable non-invasive brain stimulation," *Front. Hum. Neurosci.*, vol. 15, Jun. 2021, Art. no. 699473.

[67] O. Sharon et al., "Transcutaneous vagus nerve stimulation in humans induces pupil dilation and attenuates alpha oscillations," *J. Neurosci.*, vol. 41, no. 2, pp. 320–330, Jan. 2021.

[68] B. Lloyd et al., "Short-term transcutaneous vagus nerve stimulation increases pupil size but does not affect EEG alpha power: A replication of sharon et al. (2021, Journal of Neuroscience)," *Brain Stimulation*, vol. 16, no. 4, pp. 1001–1008, Jul. 2023.

[69] A. Pandey et al., "A 6.8W AFE for ear EEG recording with simultaneous impedance measurement for motion artifact cancellation," in *Proc. 2022 IEEE Custom Integr. Circuits Conf.*, Apr. 2022, pp. 1–2.

[70] J. Yin et al., "Motion artefact management for soft bioelectronics," *Nat. Rev. Bioeng.*, vol. 2, no. 7, pp. 541–558, Jul. 2024.

[71] X. Zhao et al., "Permanent fluidic magnets for liquid bioelectronics," *Nat. Mater.*, vol. 23, no. 5, pp. 703–710, May 2024.

[72] A. Cömert and J. Hyttinen, "Investigating the possible effect of electrode support structure on motion artifact in wearable bioelectric signal monitoring," *BioMed. Eng. OnLine*, vol. 14, no. 1, May 2015, Art. no. 44.

[73] X. Zhao et al., "A reconfigurable and conformal liquid sensor for ambulatory cardiac monitoring," *Nat. Commun.*, vol. 15, no. 1, Oct. 2024, Art. no. 8492.

[74] S. Vogel et al., "A system for assessing motion artifacts in the signal of a micro-optic in-ear vital signs sensor," in *Proc. 30th Annu. Int. Conf. IEEE Eng. Med. Biol. Soc.*, Aug. 2008, pp. 510–513.

[75] A. Ferlini et al., "In-ear PPG for vital signs," *IEEE Pervasive Comput.*, vol. 21, no. 1, pp. 65–74, Jan. 2022.

[76] K. Budidha and P. A. Kyriacou, "In vivo investigation of ear canal pulse oximetry during hypothermia," *J. Clin. Monit. Comput.*, vol. 32, no. 1, pp. 97–107, Feb. 2018.

[77] D. J. C. Matthies et al., "EarFieldSensing: A novel in-ear electric field sensing to enrich wearable gesture input through facial expressions," in *Proc. 2017 CHI Conf. Hum. Factors Comput. Syst.*, May 2017, pp. 1911–1922.

[78] A. Paul et al., "Electrode-skin impedance characterization of in-ear electrophysiology accounting for cerumen and electrodermal response," in *Proc. 9th Int. IEEE/EMBS Conf. Proc. Neural Eng.*, Mar. 2019, pp. 855–858.

[79] S. L. Kappel and P. Kidmose, "Study of impedance spectra for dry and wet EarEEG electrodes," in *Proc. 37th Annu. Int. Conf. IEEE Eng. Med. Biol. Soc.*, Aug. 2015, pp. 3161–3164.

[80] N. M. M. Noor and M. A. M. Mustafa, "Eye movement activity that affected the eye signals using electrooculography (EOG) technique," in *Proc. 6th IEEE Int. Conf. Control Syst., Comput. Eng.*, Nov. 2016, pp. 91–95.

[81] M. G. Bleichner and S. Debener, "Concealed, unobtrusive ear-centered EEG acquisition: CEEGrids for transparent EEG," *Front. Hum. Neurosci.*, vol. 11, Apr. 2017, Art. no. 163.

[82] M. S. Lee et al., "Characterization of Ag/AgCl dry electrodes for wearable electrophysiological sensing," *Front. Electron.*, vol. 2, Jan. 2022, Art. no. 700363.

[83] S. L. Kappel and P. Kidmose, "Characterization of dry-contact EEG electrodes and an empirical comparison of Ag/AgCl and IrO2 electrodes," in *Proc. 44th Annu. Int. Conf. IEEE Eng. Med. Biol. Soc.*, Jul. 2022, pp. 3127–3130.

[84] Y. M. Chi et al., "Dry-contact and noncontact biopotential electrodes: Methodological review," *IEEE Rev. Biomed. Eng.*, vol. 3, pp. 106–119, 2010.

[85] P. Kidmose et al., "A study of evoked potentials from Ear-EEG," *IEEE Trans. Biomed. Eng.*, vol. 60, no. 10, pp. 2824–2830, Oct. 2013.

[86] M. Chiu et al., "Mobile switch control using auditory and haptic steady state response in Ear-EEG," in *Proc. 9th IEEE Annu. Ubiquitous Comput., Electron. Mobile Commun. Conf.*, Nov. 2018, pp. 1032–1037.

[87] U. Ha and H.-J. Yoo, "An EEG-NIRS ear-module SoC for wearable drowsiness monitoring system," in *Proc. 2016 IEEE Asian Solid-State Circuits Conf.*, Nov. 2016, pp. 193–196.

[88] J. H. Lee et al., "CNT/PDMS-based canal-typed ear electrodes for inconspicuous EEG recording," *J. Neural Eng.*, vol. 11, no. 4, Jun. 2014, Art. no. 046014.

[89] A. R. Bertelsen et al., "Generic dry-contact Ear-EEG," in *Proc. 41st Annu. Int. Conf. IEEE Eng. Med. Biol. Soc.*, Jul. 2019, pp. 5552–5555.

[90] N. Kaongoen and S. Jo, "An auditory P300-based brain-computer interface using Ear-EEG," in *Proc. 6th Int. Conf. Brain- Comput. Interface*, Jan. 2018, pp. 1–4.

[91] R. Kaveh et al., "Wireless user-generic ear EEG," *IEEE Trans. Biomed. Circuits Syst.*, vol. 14, no. 4, pp. 727–737, Aug. 2020.

[92] D.-H. Jeong et al., "Identification of attention state for menu-selection using in-ear EEG recording," in *Proc. 5th Int. Winter Conf. Brain-Comput. Interface*, Jan. 2017, pp. 112–114.

[93] P. Kidmose et al., "Auditory evoked responses from Ear-EEG recordings," in *Proc. 2012 Annu. Int. Conf. IEEE Eng. Med. Biol. Soc.*, Aug. 2012, pp. 586–589.

[94] E. Kuatsjah et al., "Two-channel in-ear EEG system for detection of visuomotor tracking state: A preliminary study," *Med. Eng. Phys.*, vol. 68, pp. 25–34, Jun. 2019.

[95] K. B. Mikkelsen et al., "Automatic sleep staging using ear-EEG," *BioMedical Eng. OnLine*, vol. 16, no. 1, Sep. 2017, Art. no. 111.

[96] C. B. Christensen et al., "Toward EEG-Assisted hearing aids: Objective threshold estimation based on Ear-EEG in subjects with sensorineural hearing loss," *Trends Hear.*, vol. 22, Jan. 2018, Art. no. 2331216518816203.

[97] H. Liang et al., "Development and characterization of a dry Ear-EEG sensor with a generic flexible earpiece," *IEEE Trans. Instrum. Meas.*, vol. 72, 2023, Art. no. 4006212.

[98] N. Merrill et al., "One-step, three-factor passthought authentication with custom-fit, in-ear EEG," *Front. Neurosci.*, vol. 13, Apr. 2019, Art. no. 447553.

[99] D.-H. Jeong and J. Jeong, "In-ear EEG based attention state classification using echo state network," *Brain Sci.*, vol. 10, no. 6, Jun. 2020, Art. no. 321.

[100] C. Athavipach et al., "A wearable in-ear EEG device for emotion monitoring," *Sensors*, vol. 19, no. 18, 2019, Art. no. 4014.

[101] E. D. Schroeder et al., "Wearable ear EEG for brain interfacing," *Neural Imag. Sens.*, vol. 10051, pp. 110–115, Feb. 2017.

[102] S. Mandekar et al., "Advancing towards ubiquitous EEG, correlation of in-ear EEG with forehead EEG," *Sensors*, vol. 22, no. 4, Art. no. 1568, Jan. 2022.

[103] M. Pacharra et al., "Concealed around-the-ear EEG captures cognitive processing in a visual simon task," *Front. Hum. Neurosci.*, vol. 11, Jun. 2017, Art. no. 290.

[104] S. L. Kappel et al., "Reference configurations for ear-EEG steady-state responses," in *Proc. 38th Annu. Int. Conf. IEEE Eng. Med. Biol. Soc.*, Aug. 2016, pp. 5689–5692.

[105] M. G. Bleichner et al., "Identifying auditory attention with ear-EEG: CEEGrid versus high-density cap-EEG comparison," *J. Neural Eng.*, vol. 13, no. 6, Dec. 2016, Art. no. 066004.

[106] G. Hammour et al., "Hearables: Feasibility and validation of in-ear electrocardiogram," in *Proc. 41st Annu. Int. Conf. IEEE Eng. Med. Biol. Soc.*, Jul. 2019, pp. 5777–5780.

[107] T. Nakamura et al., "In-ear EEG biometrics for feasible and readily collectable real-world person authentication," *IEEE Trans. Inf. Forensics Secur.*, vol. 13, no. 3, pp. 648–661, Mar. 2018.

[108] K. B. Mikkelsen et al., "On the keyhole hypothesis: High mutual information between ear and scalp EEG," *Front. Hum. Neurosci.*, vol. 11, Jun. 2017, Art. no. 341.

[109] S. Ha et al., "Silicon-integrated high-density electrocortical interfaces," *Proc. IEEE*, vol. 105, no. 1, pp. 11–33, Jan. 2017.

[110] Y. Gu et al., "Comparison between scalp EEG and behind-the-ear EEG for development of a wearable seizure detection system for patients with focal epilepsy," *Sensors*, vol. 18, no. 1, Jan. 2018, Art. no. 29.

[111] M. T. Knierim et al., "A systematic comparison of high-end and low-cost EEG amplifiers for concealed, around-the-ear EEG recordings," *Sensors*, vol. 23, no. 9, Jan. 2023, Art. no. 4559.

[112] K. B. Mikkelsen et al., "EEGs vary less between lab and home locations than they do between people," *Front. Comput. Neurosci.*, vol. 15, Feb. 2021, Art. no. 565244.

[113] M. Bleichner, "cEEGrid EEGLAB plugin," Feb. 2022, doi: 10.5281/zenodo.5946874.

[114] A. Delorme and S. Makeig, "EEGLAB: An open source toolbox for analysis of single-trial EEG dynamics including independent component analysis," *J. Neurosci. Methods*, vol. 134, no. 1, pp. 9–21, Mar. 2004.

[115] B. Venema et al., "In-ear photoplethysmography for mobile cardiorespiratory monitoring and alarming," in *Proc. IEEE 12th Int. Conf. Wearable Implantable Body Sensor Netw.*, Jun. 2015, pp. 1–5.

[116] S. Passler et al., "In-ear pulse rate measurement: A valid alternative to heart rate derived from electrocardiography?," *Sensors*, vol. 19, no. 17, Jan. 2019, Art. no. 3641.

[117] H. J. Davies et al., "In-ear SpO2: A tool for wearable, unobtrusive monitoring of core blood oxygen saturation," *Sensors*, vol. 20, no. 17, Jan. 2020, Art. no. 4879.

[118] H. Tian et al., "Hearables: Heart rate variability from ear electrocardiogram and ear photoplethysmogram (Ear-ECG and Ear-PPG)," in *Proc. 45th Annu. Int. Conf. IEEE Eng. Med. Biol. Soc.*, Jul. 2023, pp. 1–5.

[119] N. Bui et al., "eBP: A wearable system for frequent and comfortable blood pressure monitoring from user's ear," in *Proc. 25th Annu. Int. Conf. Mobile Comput. Netw.*, Oct. 2019, pp. 1–17.

[120] G. Hammour and D. P. Mandic, "An in-ear PPG-Based blood glucose monitor: A proof-of-concept study," *Sensors*, vol. 23, no. 6, Jan. 2023, Art. no. 3319.

[121] H. J. Davies et al., "In-ear SpO_2 for classification of cognitive workload," *IEEE Trans. Cogn. Devel. Syst.*, vol. 15, no. 2, pp. 950–958, Jun. 2023.

[122] M. Lueken et al., "Photoplethysmography-based in-ear sensor system for identification of increased stress arousal in everyday life," in *Proc. IEEE 14th Int. Conf. Wearable Implantable Body Sensor Netw.*, May 2017, pp. 83–86.

[123] J. Romero et al., "OptiBreathe: An earable-based PPG system for continuous respiration rate, breathing phase, and tidal volume monitoring," in *Proc. 25th Int. Workshop Mobile Comput. Syst. Appl.*, Feb. 2024, pp. 99–106.

[124] P. Schilk et al., "VitalPod: A low power in-ear vital parameter monitoring system," in *Proc. 18th Int. Conf. Wireless Mobile Comput., Netw. Commun.*, Oct. 2022, pp. 94–99.

[125] K. Taniguchi and A. Nishikawa, "Earable POCER: Development of a point-of-care ear sensor for respiratory rate measurement," *Sensors*, vol. 18, no. 9, Sep. 2018, Art. no. 3020.

[126] M. Bermond et al., "Reducing racial bias in SpO_2 estimation: The effects of skin pigmentation," in *Proc. 45th Annu. Int. Conf. IEEE Eng. Med. Biol. Soc.*, Jul. 2023.

[127] F. Heydari et al., "Continuous cuffless blood pressure measurement using body sensors," in *Proc. 2018 IEEE SENSORS*, Oct. 2018, pp. 1–4.

[128] Q. Zhang et al., "A machine learning-empowered system for long-term motion-tolerant wearable monitoring of blood pressure and heart rate with Ear-ECG/PPG," *IEEE Access*, vol. 5, pp. 10547–10561, 2017.

[129] M. Żyliński et al., "Hearables: In-ear multimodal data fusion for robust heart rate estimation," *BioMedInformatics*, vol. 4, no. 2, pp. 911–920, Jun. 2024.

[130] H. Ota et al., “3D printed “earable” smart devices for real-time detection of core body temperature,” *ACS Sensors*, vol. 2, no. 7, pp. 990–997, Jul. 2017.

[131] D. Cárdenas-García and E. Méndez-Lango, “Blackbody for metrological control of ear thermometers,” *Proc. AIP Conf. Proc.*, vol. 1552, no. 1, pp. 976–980, Sep. 2013.

[132] J. S. Chaglla E et al., “Measurement of core body temperature using graphene-inked infrared thermopile sensor,” *Sensors*, vol. 18, no. 10, Oct. 2018, Art. no. 3315.

[133] L. B. Baker, “Physiology of sweat gland function: The roles of sweating and sweat composition in human health,” *Temperature*, vol. 6, no. 3, pp. 211–259, Jul. 2019.

[134] M. Mozaffari et al., “Anatomy and development of the mammalian external auditory canal: Implications for understanding canal disease and deformity,” *Front. Cell Devlop. Biol.*, vol. 8, Jan. 2021, Art. no. 617354.

[135] B. Gil et al., “A smart wireless ear-worn device for cardiovascular and sweat parameter monitoring during physical exercise: Design and performance results,” *Sensors*, vol. 19, no. 7, Jan. 2019, Art. no. 1616.

[136] K. Toma et al., “External ears for non-invasive and stable monitoring of volatile organic compounds in human blood,” *Sci. Rep.*, vol. 11, no. 1, Jun. 2021, Art. no. 10415.

[137] J. Kim et al., “Wearable biosensors for healthcare monitoring,” *Nat. Biotechnol.*, vol. 37, no. 4, pp. 389–406, Apr. 2019.

[138] K. Mahato and J. Wang, “Electrochemical sensors: From the bench to the skin,” *Sensors Actuators B: Chem.*, vol. 344, Oct. 2021, Art. no. 130178.

[139] L. W. Andersen et al., “Etiology and therapeutic approach to elevated lactate levels,” *Mayo Clinic Proc.*, vol. 88, no. 10, pp. 1127–1140, Oct. 2013.

[140] G. Yang et al., “Wearable device for continuous sweat lactate monitoring in sports: A narrative review,” *Front. Physiol.*, vol. 15, Apr. 2024, Art. no. 1376801.

[141] J. R. Sempionatto et al., “Touch-based fingertip blood-free reliable glucose monitoring: Personalized data processing for predicting blood glucose concentrations,” *ACS Sensors*, vol. 6, no. 5, pp. 1875–1883, May 2021.

[142] W. Tang et al., “Touch-based stressless cortisol sensing,” *Adv. Mater.*, vol. 33, no. 18, 2021, Art. no. 2008465.

[143] S. Anastasova et al., “A wearable multisensing patch for continuous sweat monitoring,” *Biosensors Bioelectron.*, vol. 93, pp. 139–145, Jul. 2017.

[144] L. Yin et al., “Wearable E-skin microgrid with battery-based, self-regulated bioenergy module for epidermal sweat sensing,” *Adv. Energy Mater.*, vol. 13, no. 4, 2023, Art. no. 2203418.

[145] A. Marques-Deak et al., “Measurement of cytokines in sweat patches and plasma in healthy women: Validation in a controlled study,” *J. Immunological Methods*, vol. 315, no. 1, pp. 99–109, Aug. 2006.

[146] D. Sim et al., “Biomarkers and detection platforms for human health and performance monitoring: A review,” *Adv. Sci.*, vol. 9, no. 7, 2022, Art. no. 2104426.

[147] J. Heikenfeld et al., “Wearable sensors: Modalities, challenges, and prospects,” *Lab Chip*, vol. 18, no. 2, pp. 217–248, Jan. 2018.

[148] A. J. Bandodkar et al., “Wearable chemical sensors: Present challenges and future prospects,” *ACS Sensors*, vol. 1, no. 5, pp. 464–482, May 2016.

[149] K. Mahato et al., “Fundamentals and commercial aspects of nanobiosensors in point-of-care clinical diagnostics,” *3 Biotech*, vol. 8, no. 3, Feb. 2018, Art. no. 149.

[150] T. Saha et al., “Wearable electrochemical glucose sensors in diabetes management: A comprehensive review,” *Chem. Rev.*, vol. 123, no. 12, pp. 7854–7889, Jun. 2023.

[151] A. Kumar and K. Mahato, “Recent advancements in bioreceptors and materials for biosensors,” in *Biosensors in Precision Medicine*, L. C. Brazaca and J. R. Sempionatto, Eds., Amsterdam, the Netherlands: Elsevier, Jan. 2024, ch. 6, pp. 163–202.

[152] H. Mirzajani et al., “An ultra-compact and wireless tag for battery-free sweat glucose monitoring,” *Biosensors Bioelectron.*, vol. 213, Oct. 2022, Art. no. 114450.

[153] J.-M. Moon et al., “Self-testing of ketone bodies, along with glucose, using touch-based sweat analysis,” *ACS Sensors*, vol. 7, no. 12, pp. 3973–3981, Dec. 2022.

[154] J. R. Sempionatto et al., “An epidermal patch for the simultaneous monitoring of haemodynamic and metabolic biomarkers,” *Nature Biomed. Eng.*, vol. 5, no. 7, pp. 737–748, Jul. 2021.

[155] J. R. Sempionatto et al., “Wearable chemical sensors for biomarker discovery in the omics era,” *Nat. Rev. Chem.*, vol. 6, no. 12, pp. 899–915, Dec. 2022.

[156] R. Lotfi et al., “A comparison between audio and IMU data to detect chewing events based on an earable device,” in *Proc. 11th Augmented Hum. Int. Conf.*, May 2020, pp. 1–8.

[157] Y. Cao et al., “CanalScan: Tongue-jaw movement recognition via ear canal deformation sensing,” in *Proc. IEEE INFOCOM 2021 - IEEE Conf. Comput. Commun.*, May 2021, pp. 1–10.

[158] P. Zhu et al., “CHAR: Composite head-body activities recognition with a single earable device,” in *Proc. 2023 IEEE Int. Conf. Pervasive Comput. Commun.*, Mar. 2023, pp. 212–221.

[159] A. Ferlini et al., “Head motion tracking through in-ear wearables,” in *Proc. 1st Int. Workshop Earable Comput.*, Feb. 2020, pp. 8–13.

[160] D. Verma et al., “ExpressEar: Sensing fine-grained facial expressions with earables,” *Proc. ACM Interact. Mob. Wearable Ubiquitous Technol.*, vol. 5, no. 3, pp. 1–129, Sep. 2021.

[161] M. Radhakrishnan et al., “Applying “earable” inertial sensing for real-time head posture detection,” in *Proc. 2021 IEEE Int. Conf. Pervasive Comput. Commun. Workshops Affiliated Events*, Mar. 2021, pp. 176–181.

[162] L. Atallah et al., “Gait asymmetry detection in older adults using a light ear-worn sensor,” *Physiol. Meas.*, vol. 35, no. 5, Apr. 2014, Art. no. N29.

[163] N. Nguyen et al., “A scalable and domain adaptive respiratory symptoms detection framework using earables,” in *Proc. 2021 IEEE Int. Conf. Big Data*, Dec. 2021, pp. 5620–5625.

[164] T. Röddiger et al., “Towards respiration rate monitoring using an in-ear headphone inertial measurement unit,” in *Proc. 1st Int. Workshop Earable Comput.*, Feb. 2020, pp. 48–53.

[165] K.-J. Butkow et al., “hEARt: Motion-resilient heart rate monitoring with in-ear microphones,” in *Proc. 2023 IEEE Int. Conf. Pervasive Comput. Commun.*, Mar. 2023, pp. 200–209.

[166] Y. Cao et al., “EarAcE: Empowering versatile acoustic sensing via earable active noise cancellation platform,” *Proc. ACM Interact. Mobile Wearable Ubiquitous Technol.*, vol. 7, no. 2, pp. 1–47, Jun. 2023.

[167] N. Oishi et al., “Detecting freezing of gait with earables trained from VR motion capture data,” in *Proc. 2021 ACM Int. Symp. Wearable Comput.*, Sep. 2021, pp. 33–37.

[168] W. Sun et al., “TeethTap: Recognizing discrete teeth gestures using motion and acoustic sensing on an earpiece,” in *Proc. 26th Int. Conf. Intell. User Interfaces*, 2021, pp. 161–169.

[169] D. Moschina et al., “Vertical jump test using an earable accelerometer,” in *Proc. Adjunct Proc. 2023 ACM Int. Joint Conf. Pervasive Ubiquitous Comput. 2023 ACM Int. Symp. Wearable Comput.*, Oct. 2023, pp. 324–326.

[170] C. P. Burgos et al., “In-ear accelerometer-based sensor for gait classification,” *IEEE Sensors J.*, vol. 20, no. 21, pp. 12895–12902, Nov. 2020.

[171] C. Hu et al., “BreathPro: Monitoring breathing mode during running with earables,” *Proc. ACM Interact. Mob. Wearable Ubiquitous Technol.*, vol. 8, no. 2, pp. 1–25, May 2024.

[172] K. Tamura et al., “PDR with head swing detection only using hearable device,” in *Proc. Adjunct 2019 ACM Int. Joint Conf. Pervasive Ubiquitous Comput. Proc. 2019 ACM Int. Symp. Wearable Comput.*, 2019, pp. 843–848.

[173] F. Germini et al., “Accuracy and acceptability of wrist-wearable activity-tracking devices: Systematic review of the literature,” *J. Med. Internet Res.*, vol. 24, no. 1, Jan. 2022, Art. no. e30791.

[174] S. Tedesco et al., “Accuracy of consumer-level and research-grade activity trackers in ambulatory settings in older adults,” *PLoS One*, vol. 14, no. 5, May 2019, Art. no. e0216891.

[175] D. M. Peters et al., “Utilization of wearable technology to assess gait and mobility post-stroke: A systematic review,” *J. NeuroEng. Rehabil.*, vol. 18, no. 1, Apr. 2021, Art. no. 67.

[176] G. M. Hammour and D. P. Mandic, “Hearables: Making sense from motion artefacts in Ear-EEG for real-life human activity classification,” in *Proc. 2021 43 rd Annu. Int. Conf. IEEE Eng. Med. Biol. Soc.*, Nov. 2021, pp. 6889–6893.

[177] T. Sepanosian and O. D. Incel, “Boxing gesture recognition in real-time using earable IMUs,” in *Proc. Companion 2024 ACM Int. Joint Conf. Pervasive Ubiquitous Comput.*, Oct. 2024, pp. 673–678.

[178] H. Li and H. Hu, “Head gesture recognition combining activity detection and dynamic time warping,” *J. Imag.*, vol. 10, no. 5, May 2024, Art. no. 123.

[179] L. Jacxsens et al., “Brainstem evoked auditory potentials in tinnitus: A best-evidence synthesis and meta-analysis,” *Front. Neurol.*, vol. 13, Aug. 2022, Art. no. 941876.

[180] J. A. Henry, “Sound therapy to reduce auditory gain for hyperacusis and tinnitus,” *Amer. J. Audiol.*, vol. 31, no. 4, pp. 1067–1077, Dec. 2022.

[181] G. Tan et al., "Does vibrotactile stimulation of the auricular vagus nerve enhance working memory? A behavioral and physiological investigation," *Brain Stimulation: Basic, Transl., Clin. Res. Neuromodulation*, vol. 17, no. 2, pp. 460–468, Mar. 2024.

[182] K. Pfeiffer et al., "Is biofeedback through an intra-aural device an effective method to treat bruxism? Case series and initial experience," *Int. J. Environ. Res. Public Health*, vol. 18, no. 1, Jan. 2021, Art. no. 51.

[183] K. Montazeri et al., "Acoustic and optoacoustic stimulations in auditory brainstem response test in salicylate induced tinnitus," *Sci. Rep.*, vol. 13, no. 1, Jul. 2023, Art. no. 11930.

[184] J. A. Waxenbaum, V. Reddy, and M. Varacallo, "Anatomy, autonomic nervous system," in *Proc. StatPearls*, Treasure Island, FL: StatPearls Publishing, Jan. 2024. [Online]. Available: https://www.ncbi.nlm.nih.gov/books/NBK539845/

[185] E. T. Peuker and T. J. Filler, "The nerve supply of the human auricle," *Clin. Anatomy*, vol. 15, no. 1, pp. 35–37, 2002.

[186] E. Kaniusas et al., "Current directions in the auricular vagus nerve stimulation II–An engineering perspective," *Front. Neurosci.*, vol. 13, Jul. 2019, Art. no. 464795.

[187] E. Kaniusas et al., "Current directions in the auricular vagus nerve stimulation I–A physiological perspective," *Front. Neurosci.*, vol. 13, Aug. 2019, Art. no. 854.

[188] E. Frangos et al., "Non-invasive access to the vagus nerve central projections via electrical stimulation of the external ear: FMRI evidence in humans," *Brain Stimulation*, vol. 8, no. 3, pp. 624–636, May 2015.

[189] N. Yakunina et al., "Optimization of transcutaneous vagus nerve stimulation using functional MRI," *Neuromodulation: Technol. Neural Interface*, vol. 20, no. 3, pp. 290–300, Apr. 2017.

[190] V. Breton-Provencher et al., "Locus coeruleus norepinephrine in learned behavior: Anatomical modularity and spatiotemporal integration in targets," *Front. Neural Circuits*, vol. 15, Jun. 2021, Art. no. 638007.

[191] A. Konjusha et al., "Auricular transcutaneous vagus nerve stimulation specifically enhances working memory gate closing mechanism: A system neurophysiological study," *J. Neurosci.*, vol. 43, no. 25, pp. 4709–4724, Jun. 2023.

[192] I. G. de Gurtubay et al., "Immediate effects and duration of a short and single application of transcutaneous auricular vagus nerve stimulation on P300 event related potential," *Front. Neurosci.*, vol. 17, Mar. 2023, Art. no. 1096865.

[193] N. Verma et al., "Auricular vagus neuromodulation—A systematic review on quality of evidence and clinical effects," *Front. Neurosci.*, vol. 15, Apr. 2021, Art. no. 664740.

[194] I. G. de Gurtubay et al., "Evaluation of different vagus nerve stimulation anatomical targets in the ear by vagus evoked potential responses," *Brain Behav.*, vol. 11, no. 11, 2021, Art. no. e2343.

[195] A. D. Farmer et al., "International consensus based review and recommendations for minimum reporting standards in research on transcutaneous vagus nerve stimulation (Version 2020)," *Front. Hum. Neurosci.*, vol. 14, Mar. 2021, Art. no. 568051.

[196] B. W. Badran et al., "Neurophysiologic effects of transcutaneous auricular vagus nerve stimulation (taVNS) via electrical stimulation of the tragus: A concurrent taVNS/fMRI study and review," *Brain Stimulation*, vol. 11, no. 3, pp. 492–500, May 2018.

[197] A. N. H. Gerges et al., "Transcutaneous auricular vagus nerve stimulation modifies cortical excitability in middle-aged and older adults," *Psychophysiol.*, Apr. 2024, Art. no. e14584.

[198] T. Polak et al., "Far field potentials from brain stem after transcutaneous vagus nerve stimulation: Optimization of stimulation and recording parameters," *J. Neural Transmiss.*, vol. 116, no. 10, pp. 1237–1242, Oct. 2009.

[199] K. Hagen et al., "Influence of different stimulation parameters on the somatosensory evoked potentials of the nervus vagus—how varied stimulation parameters affect VSEP," *J. Clin. Neuriophysiol.*, vol. 31, no. 2, Apr. 2014, Art. no. 143.

[200] B. Leutzow et al., "Vagal sensory evoked potentials disappear under the neuromuscular block–an experimental study," *Brain Stimulation*, vol. 6, no. 5, pp. 812–816, Sep. 2013.

[201] T. Polak et al., "Central neural versus peripheral muscular origin of vagus somatosensory–evoked potentials," *Brain Stimulation*, vol. 7, no. 4, pp. 624–625, Jul. 2014.

[202] M. Keute et al., "No modulation of pupil size and event-related pupil response by transcutaneous auricular vagus nerve stimulation (taVNS)," *Sci. Rep.*, vol. 9, no. 1, Aug. 2019, Art. no. 11452.

[203] C. M. Warren et al., "The neuromodulatory and hormonal effects of transcutaneous vagus nerve stimulation as evidenced by salivary alpha amylase, salivary cortisol, pupil diameter, and the P3 event-related potential," *Brain Stimulation*, vol. 12, no. 3, pp. 635–642, May 2019.

[204] L. Skora et al., "Tonic and phasic transcutaneous auricular vagus nerve stimulation (taVNS) both evoke rapid and transient pupil dilation," *Brain Stimulation*, vol. 17, no. 2, pp. 233–244, Mar. 2024.

[205] A. Y. Kim et al., "Safety of transcutaneous auricular vagus nerve stimulation (taVNS): A systematic review and meta-analysis," *Sci. Rep.*, vol. 12, no. 1, Dec. 2022, Art. no. 22055.

[206] M. M. Ottaviani et al., "In vivo recordings from the human vagus nerve using ultrasound-guided microneurography," *J. Physiol.*, vol. 598, no. 17, pp. 3569–3576, 2020.

[207] J. A. Sanchez-Perez et al., "Transcutaneous auricular vagus nerve stimulation and median nerve stimulation reduce acute stress in young healthy adults: A single-blind sham-controlled crossover study," *Front. Neurosci.*, vol. 17, Sep. 2023, Art. no. 1213982.

[208] C. Kothe et al., "The lab streaming layer for synchronized multimodal recording," *bioRxiv*, Feb. 2024.

[209] S. Dasenbrock et al., "Synchronization of ear-EEG and audio streams in a portable research hearing device," *Front. Neurosci.*, vol. 16, Sep. 2022, Art. no. 904003.

[210] O. Valentin et al., "Custom-fitted in- and around-the-ear sensors for unobtrusive and on-the-go EEG acquisitions: Development and validation," *Sensors*, vol. 21, no. 9, Jan. 2021, Art. no. 2953.

[211] P. Kidmose et al., "Ear-EEG from generic earpieces: A feasibility study," in *Proc. 35th Annu. Int. Conf. IEEE Eng. Med. Biol. Soc.*, Jul. 2013, pp. 543–546.

[212] Y. Bu et al., "A flexible adhesive surface electrode array capable of cervical electroneurography during a sequential autonomic stress challenge," *Sci. Rep.*, vol. 12, no. 1, Nov. 2022, Art. no. 19467.

[213] K. B. Mikkelsen et al., "Predicting sleep classification performance without labels," in *Proc. 42nd Annu. Int. Conf. IEEE Eng. Med. Biol. Soc.*, Jul. 2020, pp. 645–648.

[214] D. Hölle et al., "Mobile ear-EEG to study auditory attention in everyday life," *Behav. Res. Methods*, vol. 53, no. 5, pp. 2025–2036, Oct. 2021.

[215] D. Hölle et al., "Real-time audio processing of real-life soundscapes for EEG analysis: ERPs based on natural sound onsets," *Front. Neuroergonomics*, vol. 3, Feb. 2022, Art. no. 793061.

[216] D. Hölle and M. G. Bleichner, "Smartphone-based ear-electroencephalography to study sound processing in everyday life," *Eur. J. Neurosci.*, vol. 58, no. 7, pp. 3671–3685, 2023.

[217] R. F. Lyon et al., "The CARFAC v2 cochlear model in MATLAB, Numpy, and JAX," Apr. 2024, *arXiv:2404.17490*.

[218] S. Verhulst et al., "Computational modeling of the human auditory periphery: Auditory-nerve responses, evoked potentials and hearing loss," *Hear. Res.*, vol. 360, pp. 55–75, Mar. 2018.

[219] H. F. Iaccarino et al., "Gamma frequency entrainment attenuates amyloid load and modifies microglia," *Nature*, vol. 540, no. 7632, pp. 230–235, Dec. 2016.

[220] A. J. Martorell et al., "Multi-sensory gamma stimulation ameliorates Alzheimer's-associated pathology and improves cognition," *Cell*, vol. 177, no. 2, pp. 256–271, Apr. 2019.

[221] M. H. Murdock et al., "Multisensory gamma stimulation promotes glymphatic clearance of amyloid," *Nature*, vol. 627, no. 8002, pp. 149–156, Mar. 2024.

[222] C. Adaikkan et al., "Gamma entrainment binds higher-order brain regions and offers neuroprotection," *Neuron*, vol. 102, no. 5, pp. 929–943, Jun. 2019.

[223] H.-J. Suk et al., "Vibrotactile stimulation at gamma frequency mitigates pathology related to neurodegeneration and improves motor function," *Front. Aging Neurosci.*, vol. 15, May 2023, Art. no. 2023.

[224] D. Chan et al., "Gamma frequency sensory stimulation in mild probable Alzheimer's dementia patients: Results of feasibility and pilot studies," *PLoS One*, vol. 17, no. 12, Dec. 2022, Art. no. e0278412.

[225] C. G. Moreira et al., "Closed-loop auditory stimulation method to modulate sleep slow waves and motor learning performance in rats," *eLife*, vol. 10, Oct. 2021, Art. no. e68043.

[226] E. Capezuti et al., "Systematic review: Auditory stimulation and sleep," *J. Clin. Sleep Med.*, vol. 18, no. 6, pp. 1697–1709, Jun. 2022.

[227] M. Garcia-Argibay et al., "Efficacy of binaural auditory beats in cognition, anxiety, and pain perception: A meta-analysis," *Psychol. Res.*, vol. 83, no. 2, pp. 357–372, Mar. 2019.

[228] M. J. Esfahani et al., "Closed-loop auditory stimulation of sleep slow oscillations: Basic principles and best practices," *Neurosci. Biobehavioral Rev.*, vol. 153, Oct. 2023, Art. no. 105379.

[229] J. Kim et al., "Competing roles of slow oscillations and delta waves in memory consolidation versus forgetting," *Cell*, vol. 179, no. 2, pp. 514–526, Oct. 2019.

[230] J. P. Woller et al., "EEG denoising during transcutaneous auricular vagus nerve stimulation across simulated, phantom and human data," *bioRxiv*, 2024.

[231] I. Rais and T. Igasaki, "Automated detection and modeling for the removal of transcutaneous auricular vagus nerve stimulation artifacts," in *Proc. 2023 IEEE Int. Biomed. Instrum. Technol. Conf.*, Nov. 2023, pp. 120–123.

[232] C. Wienke et al., "Phasic, event-related transcutaneous auricular vagus nerve stimulation modifies behavioral, pupillary, and low-frequency oscillatory power responses," *J. Neurosci.*, vol. 43, no. 36, pp. 6306–6319, Sep. 2023.

[233] H. J. Davies et al., "The deep-match framework: R-peak detection in Ear-ECG," *IEEE Trans. Biomed. Eng.*, vol. 71, no. 7, pp. 2014–2021, Jul. 2024.

[234] R. Sclocco et al., "The influence of respiration on brainstem and cardiovagal response to auricular vagus nerve stimulation: A multimodal ultrahigh-field (7T) fMRI study," *Brain Stimulation*, vol. 12, no. 4, pp. 911–921, Jul. 2019.

[235] J. C. Cerda et al., "Proof-of-concept of respiration-triggered vagus nerve stimulation to treat epilepsy," in *Proc. 2024 IEEE Int. Symp. Med. Meas. Appl.*, Jun. 2024, pp. 1–6.

[236] T. Y. Li et al., "Non-invasive recording of parasympathetic nervous system activity on auricular vagal nerve branch," in *Proc. 42nd Annu. Int. Conf. IEEE Eng. Med. Biol. Soc.*, Jul. 2020, pp. 4337–4340.

[237] A. M. Samoudi et al., "Sensitivity analysis of a numerical model for percutaneous auricular vagus nerve stimulation," *Appl. Sci.*, vol. 9, no. 3, Jan. 2019, Art. no. 540.

[238] E. Kreisberg et al., "High-resolution computational modeling of the current flow in the outer ear during transcutaneous auricular vagus nerve stimulation (taVNS)," *Brain Stimulation*, vol. 14, no. 6, pp. 1419–1430, Nov. 2021.

[239] N. Verma et al., "Microneurography as a minimally invasive method to assess target engagement during neuromodulation," *J. Neural Eng.*, vol. 20, no. 2, Apr. 2023, Art. no. 026036.

[240] A. Berthon et al., "Using neural biomarkers to personalize dosing of vagus nerve stimulation," *Bioelectron. Med.*, vol. 10, no. 1, Jun. 2024, Art. no. 15.